Publizierbarer Endbericht

gilt für Studien aus der Programmlinie Forschung

A) Project Data

General information about the project	
Short title	FloodRisk-7000
Full title	Calculating flood risk with 7000 years of flood frequency data and highly damage relevant cyclone tracks under current & future climatic conditions
Recommended form of citation	Prettenthaler, F., Albrecher, H., Bladt, M., Habsburg-Lothringen, C., Hofstätter, M., Kortschak, D., Janisch, D., Köberl, J., Lexer, A., Swierczynski, T. (2017): FloodRisk-7000 – Calculating flood risk with 7000 years of flood frequency data and highly damage relevant cyclone tracks under current & future climatic conditions. Final report.
Program (incl. year)	ACRP 8th Call (2015)
Period	15.03.2016-14.06.2018
Coordinator/Applicant	JOANNEUM RESEARCH Forschungsgesellschaft mbH
Contact person's name	Dr. Franz Prettenthaler
Contact person's address	Waagner-Biro-Straße 100, 8020 Graz
Contact person's phone number	0316 / 876-7601
Contact person's email	franz.prettenthaler@joanneum.at
Project and cooperation partners	Alfred-Wegener-Institut Helmholtz-Zentrum für Polar- und Meeresforschung (AWI), Germany Zentralanstalt für Meteorologie und Geodynamik (ZAMG), Vienna
Keywords	Flood risk, sediment data, extreme precipitation
Total project costs	321.424 €
Funding sum	299.924 €
Klimafonds-Nr	B567123
Date of creation	14.09.2018

B) Project overview

1 Kurzfassung

Motivation

Auch wenn sich Schadendaten grundsätzlich am besten zur Schätzung des Hochwasserschadenpotentials eignen, weisen sie einen entscheidenden Nachteil auf: für gewöhnlich ist ihre Verfügbarkeit auf einen vergleichsweise kurzen Zeithorizont beschränkt. Dies führt zu großen Unsicherheiten beim Schätzen des Schadenpotentials von Ereignissen mit geringer Eintrittswahrscheinlichkeit und hohem Schadenausmaß. FloodRisk-7000 zielt auf eine Verbesserung von HW-Schadenpotentialschätzungen durch Nutzung und Zusammenführung unterschiedlicher Datensätze ab, darunter Schadendaten auf Gemeindeebene, Sedimentdaten des Mondsees zu HW-Ereignissen und Daten zu Tiefdruckzugbahnen inkl. dazugehörigen maximalen 24-stündigen Niederschlagssummen. Das Projekt verfolgt folgende Ziele: (i) Verlinkung der 7.000 Jahre umfassenden Sedimentdaten zu HW-Ereignissen mit auslösenden meteorologischen Ereignissen, (ii) Verknüpfung räumlich hochaufgelöster Schadendaten mit den wahrscheinlichsten Ursachen schadwirksamer Tiefdruckzugbahnen, (iii) Berechnung langfristiger Versicherungsprämien für den aktuellen Gebäudebestand unter Einbeziehung der Informationen aus den Sedimentdaten und (iv) Berechnung des maximalen HW-Schadenpotentials und der damit verbundenen aktuarisch fairen Versicherungsprämie auf Basis zukünftiger klimatischer und sozioökonomischer Szenarien.

Aktivitäten & Methoden

Wissen über Änderungen im Auftreten von HW-Ereignissen ist für die Bewertung des zukünftigen HW-Risikos essentiell. Darum wurden die Sedimentaufzeichnungen sommerlicher (Apr.-Aug.) HW-Ereignisse im Mondsee mittels statistischer Methoden wie der Change Point (CP) Analyse untersucht. Neben einem Vergleich mit anderen HW-Datensätzen ermöglicht der CP-Ansatz u. U. auch, die HW-Häufigkeit mit klimatischen Bedingungen in Beziehung zu setzen, indem in historischen Klimaaufzeichnungen nach ähnlichen CPs gesucht wird. Eine entsprechende statistische Analyse wurde für mehrere Klimaindikatoren durchgeführt.

Um atmosphärische Muster zu identifizieren, die zu großen Sedimentablagerungen im Mondsee führen, wurden HW-Ereignisse in den Seesedimenten nachverfolgt und deren Verbindungen zu atmosphärischen Zugbahnen analysiert. Dies erfolgte mittels Erstellung eines Zugbahn-Katalogs für die europäische Region mit zehn verschiedenen Zugbahntypen, die historischen Niederschlagsereignissen in der Mondsee-Region zugeordnet wurden. Zusätzlich wurde eine Liste der Top 100 Niederschlagsereignisse erstellt, um die Niederschläge mit den sedimentären HW-Schichten in Beziehung zu setzen. Durch die ermittelte Beziehung konnten die identifizierten atmosphärischen Muster unter zukünftigen klimatischen Bedingungen untersucht und daraus Rückschlüsse auf mögliche Veränderungen im Auftreten von HW-Ereignissen gezogen werden. Diese Informationen dienten als Input für die Modellierung zukünftiger HW-Schäden.

Zwei unterschiedliche Ansätze zur HW-Schadenmodellierung wurden angewendet: ein auf Extremwertanalyse basierendes Modell ($NeRF_{EVA}$) und ein Copula-Abhängigkeitsmodell auf Basis der HORA-Zonen ($NeRF_{HORA}$). Beide Ansätze wurden bereits im Rahmen der österreichischen HW-Risikoanalyse angewendet und in FloodRisk-7000 anhand jährlicher Schadendaten auf Gemeindeebene verfeinert. Darüber hinaus wurde ein probabilistisches Verfahren entwickelt, um sedimentäre HW-Ereignisse mit tatsächlichen Schadendaten zu verknüpfen. Dieses Verfahren ermöglichte die Berücksichtigung von statistischen Eigenschaften der 7.000 Jahre umfassenden Sedimentdaten bei der Berechnung von Schadenpotentialen, Versicherungsprämien und Kapitalanforderungen. Zudem wurde die Verknüpfung genutzt, um die potenziellen Veränderungen des Auftretens von HW-Ereignissen, die sich aus Veränderungen der atmosphärischen Muster ergeben, in zukünftige Schadenpotenziale zu übersetzen.

Ergebnisse & Schlussfolgerungen

Bei der Untersuchung der 7.000-jährigen Sedimentaufzeichnungen wurde ein Erneuerungspunktprozess („*renewal point process*“) mit einem signifikanten Change Point (CP) im HW-Ereignismuster um 350 n. Chr. identifiziert. Der Prozess wechselt dort von der Überlagerung zweier Mechanismen mit den Wiederkehrperioden 5 und 50 Jahren zu 2 und 17 Jahren. Seit Beginn der verfügbaren Schadenaufzeichnungen wurde im Vergleich zum gesamten Zeitraum seit dem CP eine etwas höhere HW-Frequenz beobachtet. Da in den Sedimentdaten kein weiterer robuster CP gefunden wurde, liegt die Annahme nahe, dass sich das HW-Häufigkeitsregime seit 350 n. Chr. nicht mehr signifikant verändert hat. Unter diesem Blickwinkel könnten Schadenpotenziale, die sich lediglich aus den jüngsten Schadenerfahrungen ableiten, das tatsächliche Risiko überschätzen. Die geschätzten durchschnittlichen Schäden und Solvency-II-Kapitalerfordernisse sind beispielsweise für den Zeitraum mit verfügbaren Schadendaten um etwa 30 % höher als für den gesamten Zeitraum seit dem CP. Andererseits sind CPs an den Grenzen einer Zeitreihe schwerer zu erkennen. Somit könnte sich das HW-Häufigkeitsregime in letzter Zeit geändert haben, ohne die Möglichkeit, den entsprechenden CP in einer statistisch signifikanten Weise nachzuweisen.

Bezüglich der Treiber von HW-Ereignissen in der Mondsee-Region wurde festgestellt, dass die meisten der Top 20 Tagesniederschlagsextrema im Sommer (1961-2015) mit Zugbahnen des Typs Vb zusammenhängen, die sich in Norditalien südlich der Alpen entwickeln. Diese Top-Niederschlagsereignisse stimmen sehr gut mit dem sedimentären HW-Aufzeichnungen des Mondsees (1976-2013) überein (bis zu 80 %). Als weiteres Hauptmerkmal konnte ein bedeutendes „Cut-Off Low“ in den oberen Atmosphärenebenen identifiziert werden, das direkt über dem Alpenbogen liegt. Für die Zukunft (2051-2100 gegenüber 1956-2005) weisen fünf der sechs betrachteten RCP/Modelllauf-Kombinationen des Klimamodells ECHAM6 auf eine Zunahme von Niederschlagsextrema hin, die im Mondsee zu HW-Einträgen führen. Die folglich zu erwartenden Änderungen im durchschnittlichen jährlichen Schaden und im Solvency II-Kapitalbedarf reichen von -19 % bis +75 % (bei gleich bleibendem Gebäudebestand). Die natürliche Variabilität ist jedoch höher als die aufgrund des Klimawandels erwartete Veränderung.

2 Executive Summary

Motivation

Although damage data is in principle the kind of data most suitable to estimate flood damage potentials, it exhibits a crucial cutback: its availability is usually limited to rather short time horizons, which causes high uncertainties in estimating the damage potential of low-probability high-impact events. FloodRisk-7000 aims at improving the estimations on flood damage potentials by making use of and merging different kinds of data sets, including amongst others damage data on municipal resolution, 7,000 years of paleoflood records derived from Lake Mondsee sediments, and cyclone tracks with their related 24 hourly precipitation maxima. The project pursues the following objectives: (i) Linking paleoflood information comprising 7,000 years to triggering meteorological events, (ii) linking actual damage experience (from a spatially highly resolved damage data base) to the most likely causes of high-impact cyclones, (iii) calculating long-term insurance premiums for the current building stock, incorporating paleoflood information, and (iv) calculating the maximal flood damage potential and the associated actuarially fair insurance premiums on the basis of future climate and socio-economic scenarios.

Activities & methods

Knowledge about changes of flood occurrence patterns is important for flood risk estimation of the future. We analysed the 7,000 year summer (April to August) flood record recovered from Lake Mondsee using statistical approaches, such as change point testing. The change point approach enables a comparison to other flood records, and possibly to relate flood frequency to climatic conditions, by looking for similar change points in the historical record of the latter. Therefore, we performed a respective statistical analysis for several climate indicators.

In order to identify atmospheric patterns leading to major sediment loads in Lake Mondsee, flood events detected in the sediments of the lake were tracked and their linkages to atmospheric cyclones analysed. For this purpose, a cyclone track catalogue covering the European region and comprising ten different cyclone track types was produced. The tracks from this catalogue were assigned to historic precipitation events in the Lake Mondsee region and a list of top 100 precipitation events (aggregated daily precipitation) was created for relating precipitation to the sedimentary flood layers. The established link also allowed investigating the identified atmospheric patterns under future climatic conditions and hence drawing conclusions on potential changes in the occurrence of flood events. This information served as input for modelling future flood damage.

Two different approaches for flood damage modelling were applied in the project: a model based on extreme value analysis ($NeRF_{EVA}$) and a copula dependence model based on the HORA risk zones ($NeRF_{HORA}$). Both approaches have already been applied in the context of Austrian flood risk analysis and were refined using annual damage data at municipal level. Moreover, a probabilistic procedure was developed for linking sedimentary flood events to actual damage data. This procedure allowed considering statistical properties of up to 7,000 years of flood frequency when calculating damage potentials, insurance premiums, and capital requirements. In addition, the link was used to translate the potential changes in the occurrence of flood events – derived from changes in atmospheric patterns – into future damage potentials.

Results & conclusions

Investigating the 7,000 years of Lake Mondsee sediment records, we identified a point process of renewal type, with a significant change point of the flood occurrence pattern around 350 AD, switching from the overlay of two mechanisms of flood recurrences of 5 and 50 years before to 2 and 17 years after this change point. Since the beginning of damage record keeping, a somewhat higher flood frequency has been observed compared to the entire period after the change point. As no further robust change point has been detected in the sediment data, we may conclude that the flood frequency regime has not significantly changed again since 350 AD. From that perspective, damage potentials derived merely from recent damage experience may overestimate actual risks. Estimated average annual damage and Solvency II capital requirements are, for instance, about 30 % higher for the period with damage data available than for the entire period since the change point. On the other hand, change points are usually harder to detect at the borders of the time series. Thus, the flood frequency regime might have changed recently, without the possibility to detect the respective change point in a statistically significant way.

Regarding the atmospheric drivers of flood events in the Mondsee region, the majority of the 20 largest daily precipitation events during summer (1961-2015) were found to be related to the occurrence of type Vb cyclones which develop around Northern Italy south of the Alps. Those top precipitation events correspond very well with the sedimentary Lake Mondsee flood record (1976-2013, up to 80 %) as well. Moreover, a major Cut-Off Low at upper atmospheric levels directly located across the Alpine Range was identified as a main feature during such events. The resulting floods, which also trigger sediment deposition in Lake Mondsee, are high intensity floods, presenting highest hourly discharges and highest dis-charges lasting at least 1-3 hours. For the future (2051-2100 compared to 1956-2005), five out of six considered RCP/model-run combinations of the climate model ECHAM6 indicate an increase in the number of precipitation extremes causing flood layer deposition in Lake Mondsee. This translates into expected shifts in average annual damage and Solvency II capital requirements ranging from -19 % to +75 % (assuming no changes in building stock values). Natural variability is, however, higher than the shift expected due to climate change.

3 Background and goal

Motivation

Floods are the leading cause of economic damage from natural disasters in Austria, accounting for 70 % of total damage from natural disasters in the period 1990 to 2016 according to EM-DAT (The OFDA/CRED International Disaster Database; www.emdat.be). Due to the comparatively high threat of damage from flood events, information on the current and future damage potential is of great importance for sustainable flood risk management but also for public finances due to the mainly public Austrian risk transfer system (Catastrophe Fund). Worldwide, actuarial (i.e. insurance mathematical) estimations of damage potentials and the resulting calculations of insurance premiums are often based on damage experience comprising comparatively short time periods and few data points. When long-term climatological damage potentials are to be estimated, these limited time periods and data points are a problem for two reasons: (i) extreme – or so called "fat-tail" – events (i.e. events of low probability, but with high impact) are very likely to be underrepresented in these damage samples and (ii) estimating damage functions based on such limited time series usually requires the assumption of stationarity due to methodological matters. Both reasons give rise to significant uncertainty, also as regards the present and future flood risk damage potential for Austria. FloodRisk-7000 is motivated by the attempt to overcome these methodological shortcomings.

Objectives

FloodRisk-7000 aimed at improving the estimations on flood damage potentials by making use of and merging different kinds of data sets, including amongst others damage data on municipal resolution, 7,000 years of paleoflood records derived from Lake Mondsee sediments, and cyclone tracks with their related precipitation totals. The project mainly focused on the northern part of Austria and pursued the following objectives: (i) Linking paleoflood information comprising 7,000 years to triggering meteorological events (so-called "Vb" cyclones or the like), (ii) linking actual damage experience (from a spatially highly resolved damage data base) to the most likely causes of high-impact cyclones, (iii) calculating long-term insurance premiums for the current building stock, incorporating paleoflood information, and (iv) calculating the maximal flood damage potential and the associated actuarially fair insurance premiums on the basis of future climate and socio-economic scenarios.

4 Project content and result(s)

FloodRisk-7000 was sub-divided into five scientific work packages complemented by one work package (WP0) for project coordination and one work package (WP6) for the dissemination of results. The work flow and dependences between work packages are illustrated in Figure 1. What follows is the description of the goals, activities and key results per scientific work package.

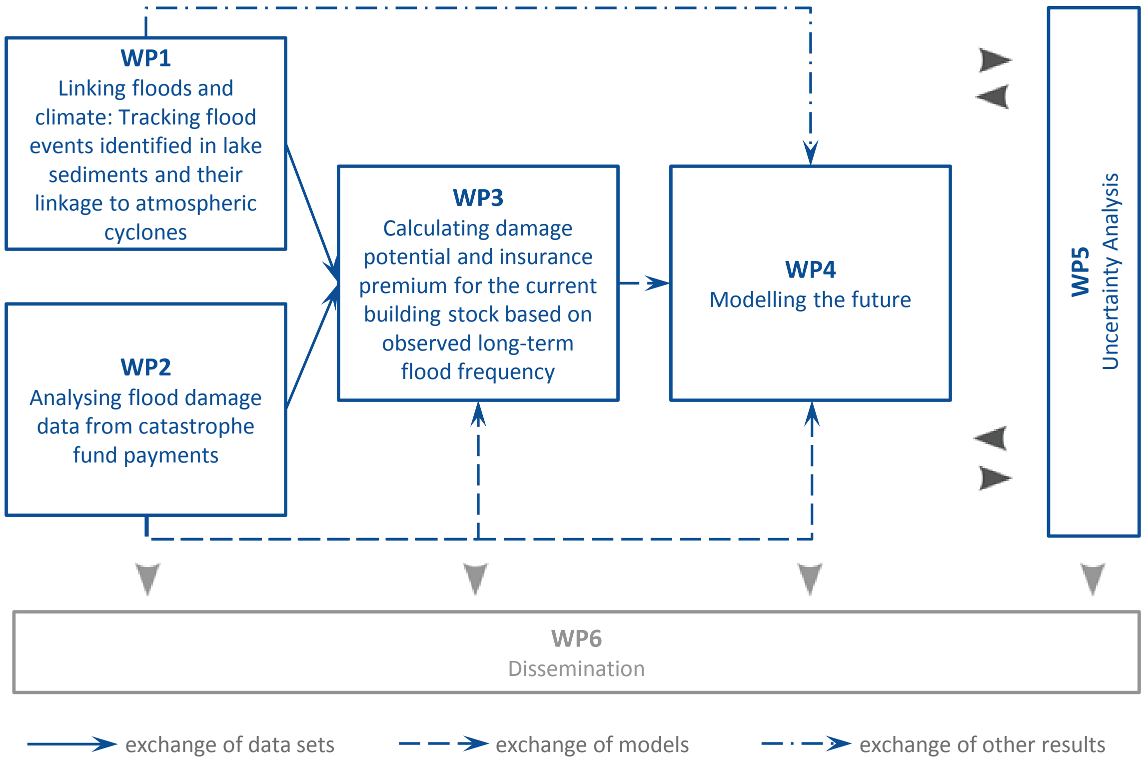

Figure 1: Work package structure and dependencies

WP1: Linking floods and climate: Tracking flood events identified in lake sediments and their linkages to atmospheric cyclones

Goals: Most disastrous floods in the NE Alps affecting large parts of Northern Austria are caused by extreme precipitation events most likely related to atmospheric cyclone tracks like Van Bebber's type Vb. WP1 aimed at understanding atmospheric cyclones, extreme precipitation and triggering flood events at Lake Mondsee as recorded in Lake Mondsee sediments within the instrumental time period 1976-2013. Sediments from Lake Mondsee reveal flood activity of the past 7,000 years reflecting summer flood activity in specific. The comparison of sediment records and advanced meteorological circulation patterns enables a better understanding of the long-term process of flood occurrence. Atmospheric patterns, which are leading to major sediment loads, can therefore be identified and investigated under future climatic conditions.

Activities: Activities within WP1 ranged from the collection and review of Lake Mondsee sediment data over the establishment of a cyclone track catalogue with corresponding precipitation totals to the linking of flood events with hydro-meteorological data.

Collection and review of Lake Mondsee sediment data: We collected data on paleoflood layers recovered from Lake Mondsee sediments (Swierczynski et al., 2012 and 2013; Kämpf et al., 2014; Lauterbach et al., 2011; unpublished datasets by GFZ). Multiple cores had been retrieved during four coring campaigns (2005, 2007, 2010, 2014) using a UWITEC gravity and piston corer in distal and proximal locations referring to the main river inflow Griesler Ache (unpublished data from the coring campaign 2014 have been communicated by GFZ Potsdam). The distal core covers 7,000 years, the proximal cores about 40 years. Lake Mondsee sediments exhibit biochemical calcite varves (annually laminated lake sediments) with intercalated detrital layers which have been deposited during runoff events (Lauterbach et al., 2011). These layers can be distinguished from the background lake sediments using combined analysis of geochemical and microfacies composition on preserved thin sections of the sediments (Lauterbach et al., 2011). According to the relative position in the varve, the flood layer season can be identified. A chronology has been established by varve counting that enables to exactly date these layers (Kämpf et al., 2014). We reviewed the available and published data for a proper use for comparison with hydro-meteorological data. For this refined analysis and comparison with instrumental data we used the time period 1976-2013 and focused on summer flood layers represented in the sediments.

Establishment of a cyclone track catalogue and calculation of related precipitation totals: In preparation for the comparison with sedimentary flood event layers, various meteorological data sets were created.

- *Cyclone track catalogue data based on JRA-55 (reanalysis) and ECHAM6 (climate model: historical and scenarios)*: The cyclone track types used in this study were identified by the classification scheme of Hofstätter et al. (2016 and 2018) developed for the European domain. Ten different track types were considered in this study, based on the geographic regions the cyclones traverse before entering Central Europe (see footnote 1 on page 11 and Table 7). The analysis was based on the Japanese 55-year reanalysis (JRA-55) of the Japanese Meteorological Agency (Kobayashi et al., 2015; Harada et al., 2016). For the analysis of future climate change (see also WP4), simulations from the global climate model (GCM) MPI-ESM-LR (Giorgetta et al., 2012; Reick et al., 2012b and 2012c) were used (run 1, 2 and 3), based on projections of atmospheric representative concentration pathways RCP4.5 and RCP8.5 (Moss et al., 2010).
- *Categorical precipitation data for region Mondsee based on SPARTACUS (1961-ongoing)*: In order to attribute individual precipitation events to track types, the 24 hourly precipitation totals (07 MEZ of the current day up to 07 MEZ of the following day) from SPARTACUS (1961-2015) were interpolated to 6 hourly precipitation sums (06, 12, 18 and 00 UTC) for the Mondsee re-

gion (R^6). R^6 was assigned to a cyclone track if that cyclone was within the "Track Recognition Zone" over Central Europe (TRZ, 0.5° E–23.9° E and 42.3° N–56.2° N) at that time. The total precipitation amount of a certain cyclone, denoted as R^{trc}, was determined by summing up precipitation (R^6) as long as a cyclone was within TRZ. In addition, we calculated the maximum 24 hourly precipitation sum (RR^{24max}) during a cyclone track event in TRZ. In order to further explore individual precipitation events, the 100 largest running 24 hourly precipitation totals (R^{24}) in the period 1961-2015 were identified. Moreover, a weighted cyclone intensity was calculated for each cyclone.

Linking of flood events with hydro-meteorological data: Daily precipitation (1961-2015) and hourly runoff events (1976-2015) were compared with flood event layers in Lake Mondsee (1976-2013) and a method for statistically determining probabilities for flood layer deposition in Lake Mondsee based on precipitation events was developed. To establish a method for estimating whether a precipitation event triggers a sedimentary deposition in Lake Mondsee or not, the top 100 list of RR^{24max} was set into relation with flood layer deposition in the lake basin. We created a simple linear model to estimate probabilities for sedimentary deposition in the lake basin both for the past (JRA-55 and ECHAM6) and for the future (ECHAM6), based on RR^{24max}.

Key results: To verify the important atmospheric mechanism for major sediment entrainments into Lake Mondsee, 100 of the largest and independent 24 hourly precipitation events were analysed in terms of the steering circulation. The events have been grouped by its rank (1-10, 11-20 and 21-100) and a composite of the upper level pressure pattern has been calculated by averaging the geopotential height anomaly (de-trended and de-seasonalised) over Europe, shown for the top 10 events in Figure 2 (left). In the middle plot of Figure 2 the according mean of the surface level pressure (SLP) field is shown with colour shading indicating vertical velocity and therefore highlighting areas with substantial lifting of moisture. Finally, the histogram of the wind direction at the surface level is shown as well (Figure 2, right) with the mean direction and mean intensity of the flow (percentile wind speed) given on top of the wind-rose.

The large scale atmospheric flow for the top 10 precipitation events at Lake Mondsee substantially differs from the events with lower ranks (see Swierczynski et al., in preparation for submission, for a comparison). As shown in Figure 2, a pronounced negative pressure anomaly is found over the Northern Adriatic Sea at Z500, indicating either a strong major trough at upper levels or even a Cut-Off Low (COL) for the top 10. It is accompanied by a strong cyclone at SLP which is located perfectly to the East of Lake Mondsee over Hungary/Slovakia. This configuration leads to a strong northerly flow against the Eastern Alps inducing a large area with enhanced vertical lifting of moisture at the northern parts of the Alpine ridge (red areas in Figure 2-mid). A very similar circulation pattern has also been found by Hofstätter et al. (2016 and 2018) and which is mostly related to the occurrence of Vb cyclone tracks. As shown in the wind-rose in Figure 2 (right), the flow at surface level is coming straight from NNE (10°) towards the Mondsee region, so perfectly perpendicular to the mountain ridge south of the lake. The flow is exceptionally strong with U_g reaching the 99th percentile as an average over 10 events. This explains the high 24 hourly precipitation amounts ranging from 67 mm to 95 mm for this group.

On the one hand the flow configuration shown in Figure 2 for the top 10 is a typical Vb-pattern, which is relatively more frequent during summer as compared to other track types (Hofstätter et al., 2016). On the other hand the atmospheric moisture content is strongly related to the temperature, so precipitation rates are usually much larger in summer, in case of Vb or other track types (Hofstätter et al., 2018). This explains the high ratio of Vb cyclones found for the top 10 events, i.e. 60 % compared to 14 % for rank 21-100 (see Swierczynski et al., in preparation for submission, for further details).

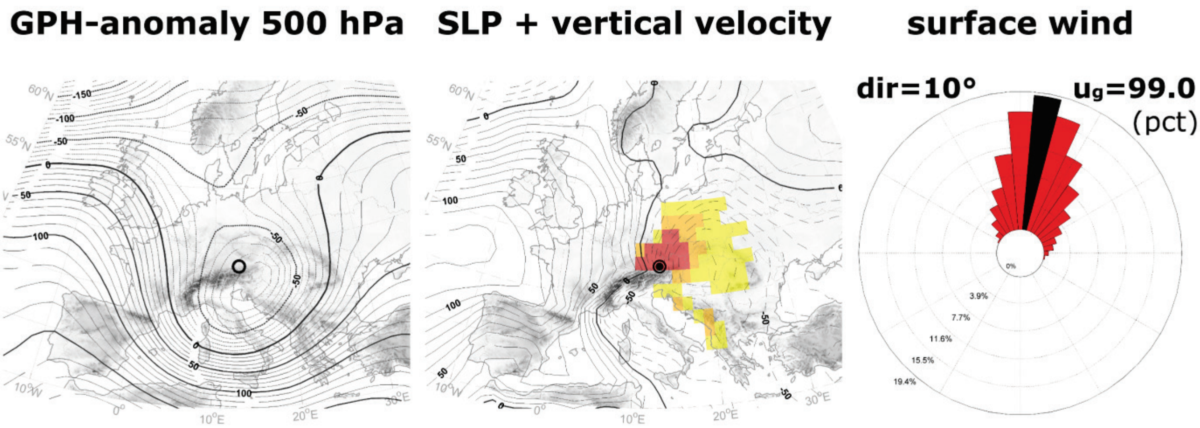

Figure 2: Analysis of the 10 largest and independent 24 hourly precipitation events in terms of the steering circulation. Left: Mean geopotential height anomaly at the pressure level of 500 hPa. Mid: Anomaly of surface level pressure shown as solid lines and with colour shading indicating vertical velocity (red=strong, yellow=weak – see Hofstätter et al., 2016 for more details). Right: Histogram of the surface wind direction with the mode shown in black and with mean direction stated on top. U_g at bottom is the average speed of surface wind but calculated from according percentiles. The circle/dot marks the Mondsee region.

Figure 3 shows the attribution of the 100 largest 24 hourly precipitation events to track types. The events were divided into winter (October to March) and summer (April to August) "half-year" to be able to identify seasonal important or dominant cyclone tracks resulting in extreme precipitation events at Lake Mondsee. Calculating the precipitation gradient in region Mondsee reveals the very important role of "Nord-Stau" situations, resulting in an increase of precipitation sums from the north towards the Alps (Figure 4), also due to orography around Lake Mondsee.

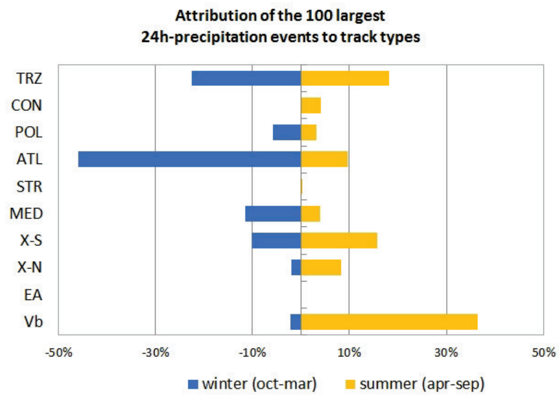

Figure 3: Top 100 precipitation events (blue: winter "half-year", yellow: summer "half-year") with cyclone track attribution.[1]

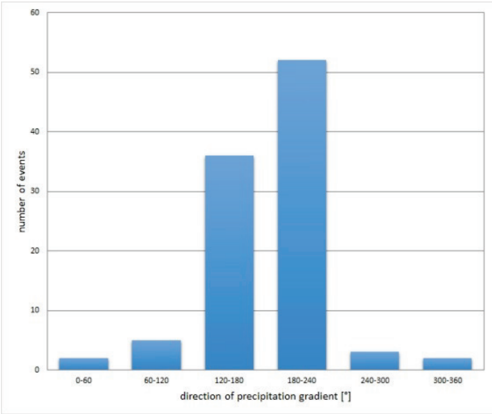

Figure 4: Precipitation gradient in region Mondsee. Abscissa: precipitation gradient classes in degree. Ordinate: number of maximum 24 hourly precipitation events from the top 100 list per class.

The comparison of extreme daily precipitation events and sedimentary flood event layers in Lake Mondsee (1976-2013) shows that nine of the top 10 daily precipitation events led to large-scale flood events which occurred in June, July and August (Table 1). Accordingly, the most recent flood events in July 1997, July 2002 and June 2013 are triggered by extreme precipitation events, which are also represented in the flood layer record of Lake Mondsee (Swierczynski et al., 2013; Kämpf et al., 2014; GFZ communication). Only one top 10 precipitation event occurred in September 2007 (71.1 mm). It has a relatively low response in hourly discharge (Q_h=57.6 m^3/s) and cannot be identified in any of the sediment cores. The 80th percentile of all precipitation events is related to daily precipitation > 72.8 mm. These daily precipitation events are related to flood events with an hourly runoff > 77.1 m^3/s. The hourly runoff of the top 10 daily precipitation extremes ranges from 70.2 to 113.7 m^3/s, except for 2007 with hourly runoff of 57.6 m^3/s.

Although the ranks of the precipitation extremes and runoff events are different (see Table 1 and Table 2), all summer flood layers in the sediment cores are represented among the top 20 events of daily precipitation and runoff extremes (i.e. 2013, 2010, 2006, 2005, 2002, 1991, 1997, 1994, 1985, 1981, and 1977). Most of the sediment layers are deposited in years corresponding to two extreme flood events. Proximal and distal sediment cores show different number of events: While flood layers in proximal cores show a higher correspondence to top 10 of daily precipitation events (80 %) and runoff events (80 %), flood layers in the distal sediment cores correspond with 40 % of top 10 precipitation events and 40 % with top 10 runoff events. For all top 10 precipitation events, however, a multicore analysis allows the identification of such non-significant flood layers in distal sediment cores and increases the correlation of flood layers with extreme precipitation and runoff events up to 80-90 %. These non-significant flood layers

[1] TRZ … All tracks emerging within TRZ (except Vb, X-N, X-S); CON … Continental; POL … Polar; ATL … Atlantic; STR … Subtropical; MED … Mediterranean; X-S … Southward propagation, emerging from the northern Adriatic Sea or Mediterranean Sea; X-N … Northward propagation, emerging from the northern Adriatic Sea or Mediterranean Sea; EA … Eastern Alpine track; Vb … van Bebber's type "five-b"

are mixed event layers or very fine-grained event layers: 2009, 2005, 1991, 1985, 1981, and 1977. Although these events are caused by an extreme daily precipitation event and show a higher hourly runoff intensity (70.2 m^3/s; 94.9 m^3/s; 84.2 m^3/s; 74.8 m^3/s; 44.8 m^3/s), very thin layers indicate either lower sediment availability in the catchment, limited lake internal processes and/or specific hydro-meteorological conditions (see also WP5 Uncertainty to sediment data). Since non-significant event layers cannot be identified using a single distal core only, flood layers which are represented in the distal core of Lake Mondsee will reflect a minimum estimation of occurring summer floods.

Table 1: Ranking of top 10 of extreme daily precipitation with related cyclone tracks (1961-2015) and flood layers in Lake Mondsee sediments (1976-2013)

Rank	Date	24h_prec_pct	24h_max_prec	Cyclone Track	Season	Sediment	Sediment	$Q_{h\ max}$
1 to 10	yyyy-mm-dd	1 = 100%	mm	Vb, EA, X-N, X-S, MED,STR, ATL, POL, CON, TRZ	Su (Apr-Aug) Wi (Sep-Mar)	Proximal cores (1976-2005)	Distal core (5145 BC - 2002 AD and additional core covering 2002-2013 [GFZ, personal communication])	m^3/s
*TOP 1-10 Precipitation events (1961-2015, * all events/annual)*								
1	1977-07-31	1,0	94,2	Vb, XS, POL, TRZ	Su	x	(x)	77,1
2	1997-07-05	0,9	86,3	Vb, X-S	Su	x	x	88,2
3	2002-08-07	0,9	84,2	X-N, ATL, POL, TRZ	Su	x	x	105,6
4	2013-06-02	0,9	82,6	CON, TRZ	Su	x	x	102,8
5	1985-08-06	0,8	76,1	Vb	Su	x	(x)	84,2
6	2002-08-12	0,8	72,8	Vb	Su	x	x	113,5
7	1981-07-19	0,8	72,8	Vb	Su	x	(x)	74,8
8	*2007-09-06*	*0,8*	*71,1*	*XS, TRZ*	*Wi*	-	-	*57,6*
9	1991-08-02	0,7	68,4	CON, TRZ	Su	x	(x)	94,9
10	2009-06-23	0,7	66,7	Vb	Su	NaN	(x)	70,2

Table 2: Ranking of top 10 of extreme hourly runoff events (1961-2015) and flood layers in Lake Mondsee sediments (1976-2013)

Rank	Date	24h_prec_pct	24h_max_prec	Cyclone Track	Season	Sediment	Sediment	$Q_{h\ max}$
1 to 10	yyyy-mm-dd	1 = 100%	mm	Vb, EA, X-N, X-S, MED,STR, ATL, POL, CON, TRZ	Su (Apr-Aug) Wi (Sep-Mar)	Proximal cores (1976-2005)	Distal core (5145 BC - 2002 AD and additional core covering 2002-2013 [GFZ, personal communication])	m^3/s
*TOP 1-10 Precipitation events (1961-2015, * all events/annual)*								
1	1977-07-31	1,0	94,2	Vb, XS, POL, TRZ	Su	x	(x)	77,1
2	1997-07-05	0,9	86,3	Vb, X-S	Su	x	x	88,2
3	2002-08-07	0,9	84,2	X-N, ATL, POL, TRZ	Su	x	x	105,6
4	2013-06-02	0,9	82,6	CON, TRZ	Su	x	x	102,8
5	1985-08-06	0,8	76,1	Vb	Su	x	(x)	84,2
6	2002-08-12	0,8	72,8	Vb	Su	x	x	113,5
7	1981-07-19	0,8	72,8	Vb	Su	x	(x)	74,8
8	*2007-09-06*	*0,8*	*71,1*	*XS, TRZ*	*Wi*	-	-	*57,6*
9	1991-08-02	0,7	68,4	CON, TRZ	Su	x	(x)	94,9
10	2009-06-23	0,7	66,7	Vb	Su	NaN	(x)	70,2

WP2: Analysing flood damage data from catastrophe fund payments

Goals: The objective of WP2 was to analyse flood damage data at municipal level for the provinces Salzburg, Upper Austria, Lower Austria and Styria. The main goal was to find a model (the distribution) for floods exceeding a certain return period or damage level to be then used within WP3 to generate synthetic time series of damage data.

Activities: WP2 activities included the collection, normalization, and modelling of flood damage data.

Collection of flood damage data: Monetary data on flood damage to buildings, building structures and inventories – owned by physical or legal persons – were collected from the provinces of Upper Austria, Lower Austria, Salzburg and Styria on a yearly and municipal resolution. The collected data results from claims for aid due to damage from catastrophic events. Depending on the province, available damage data comprises a time span of 8 (Upper Austria) to 25 years (Styria, Salzburg).

Normalization of flood damage data: By means of data on estimated building stock values per year and municipality (measured in terms of the new construction value and adjusted for inflation) the data on flood damage was normalized.

Modelling of flood damage using the $NeRF_{EVA}$[2] model: Following the standard procedure in Extreme Value Analysis (EVA) we fitted a generalized Pareto distribution to the right tail of the distribution of flood damage at municipal level. Since for individual municipalities the time series of damage data is not sufficiently long to allow for meaningful statistical analysis we chose a model where the number of parameters is reduced. Therefore we assumed that the parameters of the generalized Pareto distribution as well as the threshold (from which on the model is applied) depend on covariates (size of HQ-zones). The spatial dependence of damage between municipalities represents a challenge in the estimation procedure. Following Asadi et al. (2015), who fitted similar models for discharge data, we applied the so called independence likelihood approach (Chandler and Bate, 2007). This approach uses the density of independent random variables in the estimation process, which causes some reduction in efficiency but still leaves the estimator unbiased. Fitting the model to the damage data provided us with a marginal distribution of flood risk for each municipality. To calculate the damage for larger areas, the data needs to be aggregated. For the purpose of aggregation we used a dependence structure estimated from discharge data (see the description of the $NeRF_{HORA}$ model below for more details).

Modelling of flood damage using the $NeRF_{HORA}$[3] model: For this task we used a model already described in Prettenthaler and Albrecher (2009) and Prettenthaler et al. (2015). The principle idea of the model is to use data from hazard maps (in this case the hazard map of the HORA project) to derive marginal distributions of flood damage at municipal level. In a second step these marginal distributions are aggregated using copulas (dependence structure). The original model was enhanced in three aspects:

1. A key input parameter for the model is the average damage to a building. Within FloodRisk-7000 we estimated the damage per building using the damage data at municipal level from the four provinces Salzburg, Upper Austria, Lower Austria and Styria (instead of using figures from the literature).

[2] $NeRF_{EVA}$ … Neighbourhood Relationship Flood risk model based on Extreme Value Analysis
[3] $NeRF_{HORA}$ … Neighbourhood Relationship Flood risk model based on HORA risk zones

2. Another key input parameter for the model is the number of buildings located in different risk zones (HORA-zones). For this purpose, we disaggregated data on the built-over area (in m²) from 10 km resolution (Statistics Austria) to 10 m resolution, using satellite data on built-up area from Copernicus European Settlement Map. We assumed one building per 100 m² built-over area.
3. The time series available on flood damage at municipal level are rather short for deriving a spatial dependence structure. However, longer times series are e.g. available on discharge. Since it is arguable that damage caused by flooding is strongly related to events with extreme discharge we can assume that the spatial dependence of extreme discharge is similar to the spatial dependence of flood damage and therefore use the former as a proxy for the latter. Hence, we used data on the river network (from Copernicus) and discharge data from measurement stations (from ehyd) to estimate a max stable process for the dependence of high discharge events in river networks. The method applied is based on Asadi et al. (2015), but splits the area into different regions to account for different climate influences.

Key results: Two different methods were used within WP2 to model municipal flood damage data, i.e. Extreme Value Analysis ($NeRF_{EVA}$) and a Copula dependence model of return periods ($NeRF_{HORA}$). Table 3 and Table 4 illustrate the results of the two models for the provinces Salzburg and Upper Austria, including the estimated average annual damage and the estimated damage for events of a given return period. The calculations are based on 100,000 model runs.

Table 3: Results of $NeRF_{EVA}$ for different areas: estimated average annual damage and estimated damage for events of a given return period (in million Euros).

Region	Average	30	100	200	300	1,000
Salzburg	7.1	18	85	176	266	880
Upper Austria	12.2	22	128	265	385	1,270

Table 4: Results of $NeRF_{HORA}$ for different areas: estimated average annual damage and estimated damage for events of a given return period (in million Euros).

Region	Average	30	100	200	300	1,000
Salzburg	6.8	57	139	206	241	364
Upper Austria	14.6	111	290	443	522	890

Due to the chosen method, results for quantiles are more reliable than results for the average damage. For $NeRF_{HORA}$ the average annual damage heavily depends on the chosen interpolation between the HQ30 zone and zones with return periods of less than 30 years, for which no data is available. This problem is not that severe for the quantiles shown in Table 3 and Table 4, as we only consider return periods of 30 years and more. For the $NeRF_{EVA}$ model we use a distribution which does not have a finite variance. This makes it difficult to estimate the average damage, with a substantial part coming from single high value events. Interestingly, both methods provide very similar results on the average damage.

Regarding the quantile figures note that for $NeRF_{HORA}$ input information on flood risk zones are only available up to a return period of 200 years (zones with return periods of more than 200 years are interpolated). Since the aggregated damage of return periods exceeding 200 years are often the result of simultaneous damage in a number of municipalities – where the damage in the single municipalities may still correspond to return periods of less or around 200 years – using the model to approximate the aggregate damage for return periods of more than 200 years is nevertheless appropriate and reasonable. However, uncertainty increases the more the considered return period exceeds 200 years. For the $NeRF_{EVA}$ model we basically only have 20 years of data available for estimating the damage associated with different return periods. While the different municipalities help in getting a bit more confidence for higher quantiles, the problem remains that the difference between the number of available observations and the considered return period – and hence the associated uncertainty – is soon getting large when looking at higher return periods. Comparing the results of the two models shows a steeper increase in the quantiles resulting from $NeRF_{EVA}$ than in the quantiles resulting from $NeRF_{HORA}$. For a 200-year event, results indicate a damage of about € 200 million for Salzburg and € 350 million for Upper Austria. Overall, using two different modelling approaches helps in illustrating the scope of uncertainty related to flood risk modelling, with each approach exhibiting particular advantages and limitations.

WP3: Calculating damage potential and insurance premium for the current building stock based on observed long-term flood frequency

Goals: The objective of WP3 was to calculate the insurance premium for the current building stock (value) based on observed long-term, pre-instrumental flood frequency data derived from lake sediments extending back to 7,000 years ago.

Activities: WP3 activities included the statistical analyses of sedimentary flood layer data, the development of a model relating sedimentary flood frequency to damage data, and the calculation of insurance premiums and capital requirements based on a flood damage model that incorporates information from the sediment records.

Testing statistical properties of the long-term flood frequency derived from Lake Mondsee sediments: Several statistical tests were run on the time series of flood occurrence derived from Lake Mondsee sediment records, focusing on the inter-flood times.

- Tests for a homogeneous and inhomogeneous Poisson process underlying the observed flood occurrence time series were performed, using time transformation techniques.
- A change-point detection analysis based on both the mean and variance was carried out, as well as cumsum tests on the mean. In addition, sigmoid function fits on the series of inter-flood times were performed to study the speed

at which the regime changes, as well as regression tests that allow for co-existence of trends and change-points. Similar tests were then applied to other paleoflood records and climate indicators like the North Atlantic Oscillation (NAO).

- Auto-correlation, partial auto-correlation plots as well as empirical copula tests with varying lags in the time series were performed to detect possible dependence and persistence patterns.
- General phase-type distributions were fitted to the inter-flood times using maximum likelihood techniques via the EM algorithm.

Development of a model relating the flood frequency to actual annual claim data: Based on (i) an analysis of Lake Mondsee sediment records, (ii) discharge data from the station St. Lorenz and (iii) data on flood damage in the municipality Thalgau (Salzburg), a probabilistic procedure was developed for linking flood events derived from sediment records to damage data. The procedure allows considering statistical properties of 7,000 years of flood frequency when calculating damage potentials, insurance premiums, and capital requirements.

Calculation of insurance premiums and hypothetical capital requirements for the last 7,000 years: Using the flood damage models $NeRF_{EVA}$ and $NeRF_{HORA}$ (WP2) and the procedure developed for considering information on flood frequency from sediment data, 10,000 realizations of flood damage were simulated per considered year. These simulations formed the basis for calculating actuarially fair insurance premiums – i.e. premiums resulting in zero expected profits for the insurance company – for different time periods. Premiums resulting from the additional consideration of 7,000 years of flood frequency experience were compared to premiums resulting from considering damage data only (the latter representing the outcome of "*previous approaches*"). The 10,000 realizations of simulated flood damage also served as a basis for calculating the Solvency II capital requirements for the last 7,000 years, assuming the current building stock value for the entire period.

Key results: The performed tests for a homogeneous or inhomogeneous Poisson process underlying the observed flood occurrence time series of Lake Mondsee (7,000 years of sediment records) were amply rejected. Hence, a Poisson process cannot account for the variability and clustering observed in the data. However, we identified a point process of renewal type, with a significant change point of the flood occurrence pattern around 350 AD, switching from the overlay of two mechanisms of flood recurrences of 5 and 50 years before to 2 and 17 years after this change point. The pertinence of the result is underlined by a regression fit based on GLM techniques as well as sigmoid fits, indicating a sharp change rather than a continuous trend. This information was used in the subsequent modelling of the flood damage potential.

The following probabilistic procedure was developed for linking flood events derived from sediment records to damage data:

1. Estimation of the probability that "high" discharge is observed in the Griesler Ache in a particular year, i.e. that yearly maximal hourly discharge at the sta-

tion St. Lorenz (see left plot of Figure 5) exceeds 80 m³/s.

Note: from calibrating the sediment data with run offs of the Griesler Ache we know that maximum discharges exceeding ~80 m³/s usually coincide with sedimentary flood layers.

2. Calculation of the damage threshold for the municipality Thalgau. The damage threshold determines if the distribution for large or small damage is used subsequently. The damage threshold is calculated as Value at Risk (VaR), based on the probability of "high" discharge (i.e. > 80 m³/s) at the station St. Lorenz, using $NeRF_{EVA}$ or $NeRF_{HORA}$. I.e., we determine the damage amount that shows the same probability as "high" discharge.

   Note: available monetary data on flood damage only comprises eight years for municipalities in Upper Austria, but 25 years for municipalities in Salzburg. That is why we used damage data of the municipality Thalgau (Salzburg) instead of damage data of the municipality St. Lorenz (Upper Austria) in the described procedure. Note further that the match between sediment data, discharge data and damage data with respect to flood occurrence is good but not perfect. Damage might for example be reported in a year without sedimentary flood layer and/or without maximal discharge exceeding 80 m³/s. That is why the described procedure considers separate distributions for small and for large damage.

3. Estimation of the conditional probability distribution of damage for municipalities in the "Mondsee region" (see right plot of Figure 5) given that the damage in Thalgau is above or below the threshold calculated in step 2.

   Note: The "Mondsee region" is defined as the region that shows similar discharge extremes as station St. Lorenz.

4. Estimation of the probability that a flood event according to the sediment records is associated with "high" discharge in St. Lorenz. This gives us a stochastic link between sediment records and damage data. Using this link, insights about the event distribution gained from the 7,000 years of sediment records can be considered when estimating the damage potential.

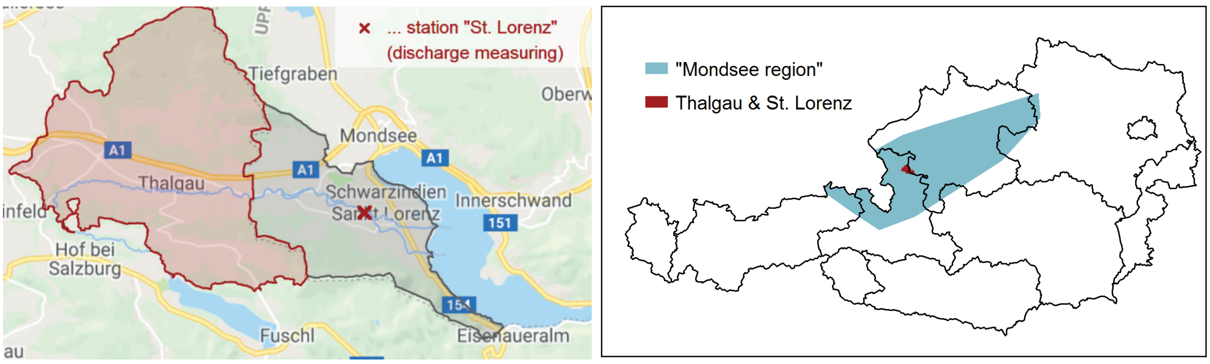

Figure 5: Location of the measurement station St. Lorenz (left) and delineation of the region with similar discharge extremes (right). Map data © 2017 GeoBasis-DE/BKG (© 2009), Google.

With the described method a hypothetical damage amount can be simulated for each of the 7,000 years of sediment records, where the damage amount depends on the occurrence (yes/no) of a flood layer in the sediment records. Note that the sediment records do not provide any information on flood severity, but only on flood frequency. Hence, we did not assume any changes in flood severity over time. However, as flood frequency changes over time, return levels change as well.

Figure 6 shows the average annual damage (i.e. the fair premium) and the damage of a 200 year event (i.e. the 99.5 % VaR or Solvency II capital requirement) for the "Mondsee region", when considering the information on flood frequencies from the sediment records ("with SR"). Both indicators were calculated for different time periods of the available 7,000 years of sediment records: the complete time span, the time before respectively after the change point (CP) at 350 AD (see T3.1), and the last 100 years. In addition, Figure 6 illustrates the results for the approach that does not take the information on flood frequencies from the sediment records into account ("without SR"). The latter corresponds to the results of WP2, but for the "Mondsee region" instead of the selected provinces.

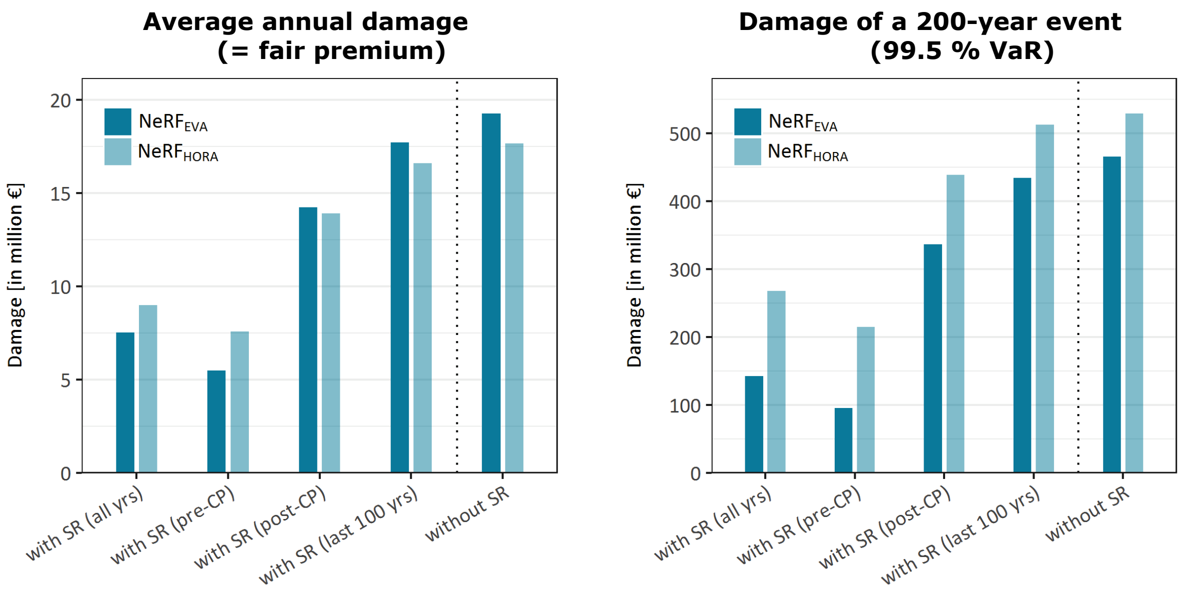

Figure 6: Estimated annual damage (left) and estimated damage of a 200-year event (right) for different constellations of sediment record consideration.

Differences between $NeRF_{EVA}$ and $NeRF_{HORA}$ are similar to WP2 results and hence not further discussed at this point. Here, we rather concentrate on comparisons between the different time periods (all years, pre-/post-CP, last 100 years) and the different approaches (with vs. without SR). Following Figure 6, the flood damage potential in the "Mondsee region" is significantly higher for the period after the change point than the period before the change point. The highest flood damage potential, however, results from the approach that only considers information from actual damage experience ("without SR"). In other words, the period, for which actual damage experience is available, shows a higher flood frequency than e.g. the last 100 years or the time period after the change point. Since we didn't detect any robust further change point in the sediment data, we may conclude that the flood frequency regime hasn't changed since 350 AD. Hence, if model calibration is limited to the time span for which data on flood damage is available, the resulting estimates are very likely to overestimate actual flood potential. On the other hand, change points are usually harder to detect at the borders of the time series. Thus, the flood frequency regime might have changed recently, without the respective change point having been detected yet.

WP4: Modelling the future

Goals: The objective of WP4 was to analyse changes in the future flood damage potential due to changes in climatic and/or socio-economic conditions.

Activities: WP4 activities included the analysis of potential changes in cyclone tracks and flood-causing heavy precipitation events in region Mondsee, the generation of different building stock value scenarios and the estimation of the future flood damage potential.

Analyses on how cyclone tracks, with a particular potential for heavy precipitation events in region Mondsee, will develop according to climate scenarios until 2100: We created a cyclone track catalogue for 2015-2100 and analysed the change of the risk of Vb. Vb cyclones are specifically relevant for major precipitation events at Lake Mondsee. So we considered Vb cyclones themselves as a risk and analysed their occurrence for the summer season, as the strongest precipitation and flood events are observed between May and October. In addition, the statistical precipitation simulation model of WP1 was used for simulating the maximum 24 hourly precipitation events for both ECHAM6 emission scenarios (RCP4.5 and RCP8.5) and all available realizations (run1, run2 and run3). Having these precipitation data, a list of the 100 largest RR^{24max} events for the period 2051-2100 was created, as for the past (1956-2005). Both lists were compared in regard to determine future change signals. In a further analysis for determining change signals, the largest 100 precipitation events were assigned to cyclone tracks with the same method as described in WP1. Afterwards these future lists (2051-2100) were compared with the historical ones (1956-2005). For future estimation on damage potential, probabilities for sedimentary deposition in Lake Mondsee on an annual basis were calculated (2051-2100). This was done with the method developed in WP1 for statistically determining probabilities for flood layer deposition in Lake Mondsee.

Generation of different scenarios on the development of the future building stock value (until 2075): Based on existing population projections and different assumptions on the construction activities in risk zones (HQ-zones), we derived five different scenarios on the evolution of the building stock value at municipal level, including a "constant building stock value"-scenario in order to study the "pure" climate change effect. With respect to population projections, we made use of the main variant of the ÖROK regional population forecast 2014 (ÖROK, 2015), which provides forecasted population figures on district level until 2075. For each municipality within a district we assumed the district's population change. Furthermore, we assumed that the relative change in a municipalities building stock (value) equals the relative change in its population. With respect to construction activities in HQ-zones, we differentiated the following four scenarios: (1) the change in the building stock (value) is uniform over all zones; (2) increases in the building stock (value) are only possible outside HQ30 zones (i.e. construction ban in HQ30 zones); (3) increases in the building stock (value) are only possible outside HQ100 (and higher) zones; (4) increases in the building stock (value) are only possible outside HQ200 (and higher) zones. Together with the "constant building stock value"-scenario, this sums up to five different scenarios on the evolution of the building stock value at municipal level.

Estimation of the future flood damage potential: Based on the probability for flood layer deposition calculated for a historic (1956-2005) and a future (2051-2100) period, we simulated the occurrence of a layer deposition (yes/no) for each year in the two periods. Using these simulated layer depositions and the procedure developed in WP3 for linking sediment records (i.e. layer depositions) and damage data, 10,000 realizations of flood damage were simulated for each year of the two considered periods. Based on these simulations, expected yearly damage and Value at Risk (VaR) figures were calculated for the historic and the future period. The method was applied on the five different building stock value scenarios, using the figures of 2075 for representing the future period.

Key results: Table 5 shows the mean annual occurrence rate of Vb cyclones at SLP for different time periods. When comparing the observed annual frequency of Vb cyclones against the simulated one (observed vs. historical), climate models appear to overestimate the rate of Vb heavily by a factor of two. When disregarding this bias for now, relative changes of Vb cyclone frequency is also shown for the future period 2051-2100 compared to 1956-2005 in Table 5. For all RCPs and throughout all model runs a decrease of -21 % to -3 % is found for Vb cyclones on an annual base (average: -14 %). Interestingly the change for RCP8.5 is similar to RCP4.5 in run3, indicating that decadal climate variability is still very large at the end of the next century and more specific comparably large as the climate change signal. This is supported by the large differences found between the different runs as well, pointing out a large internal variability for the occurrence of Vb cyclones. Such large natural long term variability can only be forced by modes of the large scale atmospheric circulation.

Table 5: Mean annual occurrence rate of Vb cyclones at SLP. Time periods used: observed (1959-2010); historical (1956-2005); RCP's (2051-2100).

	Vb summer cyclones	JRA-55	E6_run1	E6_run2	E6_run3
y^{-1}	**observed**	4.58 y^{-1}		/	
	historical	/	11.1	9.7	10.4
	RCP 4.5		9.9	9.4	8.3
	RCP 8.5		9.1	9.1	8.1
%	**Δ RCP 4.5**		-10.8	-3.3	-20.7
	Δ RCP 8.5		-18.5	-6.6	-21.6

Comparing the top 100 simulated RR^{24max} events for 2051-2100 to 1956-2005 for both ECHAM6 emission scenarios (RCP4.5 and RCP8.5) and all available realizations (run1, run2 and run3) shows a slight increase in RR^{24max} amounts for both scenarios: +3.8 % to +10.6 % for RCP8.5 and +2.0 % to +6.3 % for RCP4.5. Since previous results illustrate a mean decrease in the annual number of Vb cyclones for the future, change signals are based in the first instance on temperature changes and consequently in changes in humidity available in the atmosphere.

Figure 7 shows the climate change signal for the cyclone track contribution in the top 100 RR^{24max} events at Lake Mondsee. The left plot illustrates the results for the top 20 RR^{24max} events for all data available from ECHAM6, while the right plot shows the top 21-100. Generally speaking, there is no change in the mean number of Vb cyclones for the top 20 RR^{24max} events for both ECHAM6 scenarios (left plot of Figure 7). For the top 21-100 events RCP4.5 shows a slight decrease in Vb events and RCP8.5 shows no change in the number of Vb cyclones.

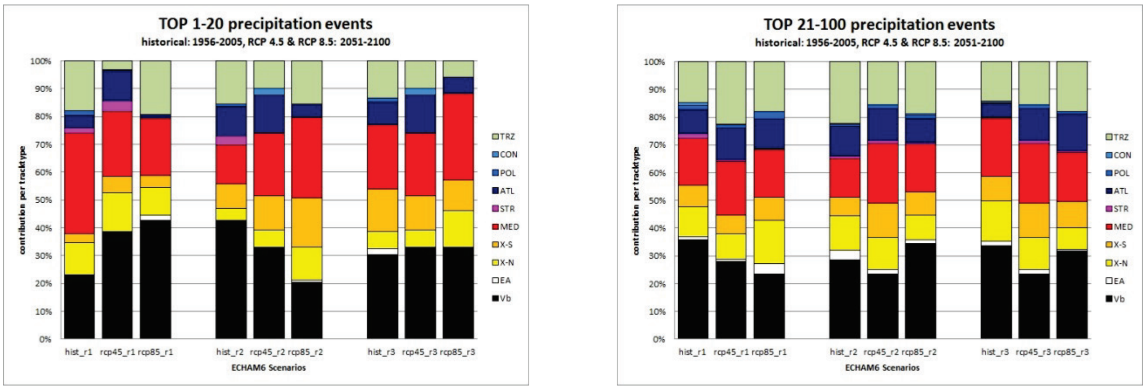

Figure 7: Climate change signal (ECHAM6) for the cyclone track contribution in the top 20 (left) and top 21-100 (right) RR^{24max} events at Lake Mondsee for the future (2051-2100).

For future estimation on damage potential, probabilities for sedimentary deposition in Lake Mondsee on an annual basis were calculated (2051-2100). This was done with method developed in WP1 for statistically determining probabilities for flood layer deposition in Lake Mondsee, using RR^{24max}. Table 6 shows the resulting average annual number of events causing flood layer deposition, based on ECHAM6. Apart from model run 2, both RCPs indicate an increase of events in the future.

Table 6: Changes in the statistically derived number of RR^{24max} events causing flood layer deposition in Lake Mondsee. Time periods: historical (1956-2005); RCP's (2051-2100).

ECHAM6	historical	RCP4.5	RCP8.5
run1	0.18	0.22 (↑)	0.22 (↑)
run2	0.20	0.17 (↓)	0.37 (↑)
run3	0.18	0.20 (↑)	0.26 (↑)

Figure 8 shows the estimated historical and future flood damage potential (average annual damage and 99.5 % VaR), based on the simulated occurrence of a flood layer deposition in each year of the two periods. Circles represent the mean over the 10,000 simulation runs, whereas error bars indicate the interval in which 95 % of all simulation runs fall. Assuming a constant building stock value, the results in Figure 8 illustrate the pure climate change effect. Hence, not surprisingly, changes in the simulated historical and future damage show the same behaviour as the derived flood event layers in Table 6. While there is no dramatic change in the mean average damage or VaR (represented by the circle) between historical and future period (the shift ranges from -19 % to +75 %), the variability of damage simulation runs within one and the same period can be quite large. There are basically two reasons for this high variability. Firstly, the distribution of flood damage is heavy tailed; hence the expected damage shows quite a big variance. Secondly, the relationship between sediment event layer and damage is modelled by a stochastic link (see WP3). For a short period like 30 years it makes a big difference if there is one additional high-damage event or not, particularly for the average annual damage. Overall, the large confidence intervals are more a consequence of the stochastic nature of the flood risk process than of the applied methods. Hence, the key statement of the results shown in Figure 8 is that natural variability is higher than the shift expected due to climate change.

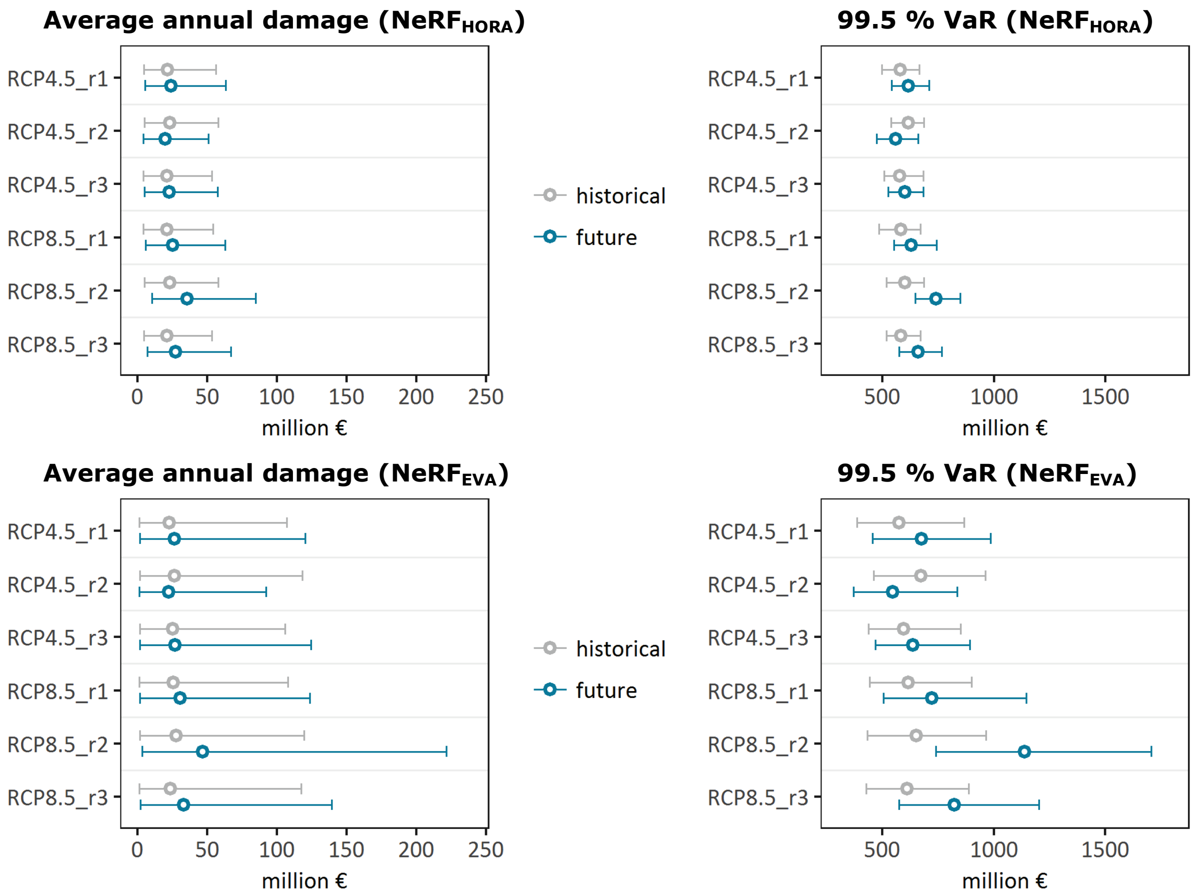

Figure 8: Historical (1956-2005) and future (2051-2100) flood damage potential, assuming a constant building stock value (i.e. pure climate change effect). Circles represent the mean of the 10,000 simulation runs; error bars the 95 % confidence intervals.

Figure 9 shows the estimated historical and future flood damage potential (average annual damage and 99.5 % VaR) for NeRF$_{HORA}$, differentiating between different building stock value scenarios. The scenario "future (constant)" refers to the constant building stock value scenario and hence displays the pure climate change effect. All future scenarios marked with a "Δ" assume a changing building stock value according to the developed scenarios. They differ with respect to the allowed construction activities in HQ-zones: whereas there are no limitations in construction activities in the "all zones" scenario, there are construction bans in the respective risk zones (and all zones of higher risk) in the scenarios "no HQxx". Expectably, the growing building stock value – as assumed in all "Δ"-scenarios – exacerbates total flood damage potential. However, the more restrictive the construction bans, the less pronounced is the exacerbation of the flood damage potential.

Whereas the assumed growth in the building stock value has a comparably small effect on the future average annual damage, it may more than double the climate change effect on the Solvency II capital (99.5 % VaR), especially if construction activities in risk zones are not regulated.

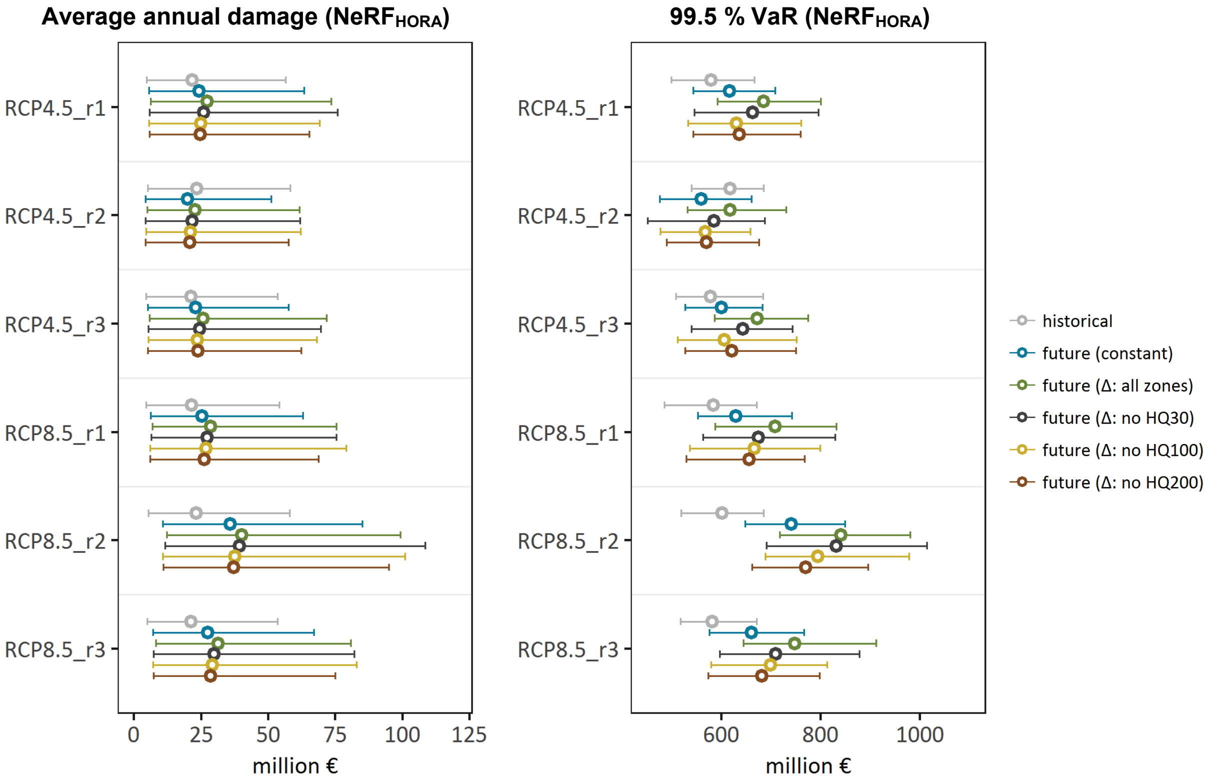

Figure 9: Historical (1956-2005) and future (2051-2100) flood damage potential for different building stock value scenarios. Circles represent the mean of the 10,000 simulation runs; error bars the 95 % confidence intervals.

WP5: Uncertainty analysis

Goal: The objective of WP5 was to analyse uncertainties throughout the modelling chain, including uncertainties related to the dating of flood events in sediment record data, uncertainties related to climate modelling as well as flood risk modelling and uncertainties arising from the interplay of the single modelling steps.

Activities: Uncertainties related to sediment record data, meteorological and climate modelling as well as flood risk modelling were described and uncertainty reductions resulting from the current modelling approach – compared to previous approaches – assessed.

Key results: As mentioned above, we identified a point process of renewal type when investigating the 7,000 years of Lake Mondsee sediment records, with a significant change point of the flood occurrence pattern around 350 AD, switching from the overlay of two mechanisms of flood recurrences of 5 and 50 years before to 2 and 17 years after this change point. Several assessments of data with lower resolution were performed to highlight the increased power of available resolution in the Lake Mondsee record. In order to compare our results with previous ones of lower resolution, where date stamps were only available at fewer places of the sediment core, we binned every three flood events into the respective time window and allowed for an additional uncertainty of three years in the dating. Redoing the analysis for this lower resolution, one could again identify one change-point in the dynamics at that same time and the fit led to a renewal model, however the resulting inter-flood distribution was now quite different leading, throughout history, to a very different expected time until the next future flood given the number of years since the last flood when compared with the full resolution result.

Overall, the uncertainty analyses performed throughout the project resulted in a much richer understanding of the natural variability in the underlying flood processes than what could have been expected from traditional flood risk modelling approaches. Therefore, the current analyses increase the perception of uncertainty beyond the state-of-the-art perception of modelling uncertainty in flood risk modelling approaches.

5 Conclusions and recommendations

Investigating the 7,000 years of Lake Mondsee sediment records, we identified a point process of renewal type, with a significant change point of the flood occurrence pattern around 350 AD, switching from the overlay of two mechanisms of flood recurrences of 5 and 50 years before to 2 and 17 years after this change point. Since the beginning of damage record keeping, a somewhat higher flood frequency has been observed compared to the entire period after the change point. As no further robust change point has been detected in the sediment data, we may conclude that the flood frequency regime has not significantly changed again since 350 AD. From that perspective, damage potentials derived merely from recent damage experience may overestimate actual risks. Estimated average annual damage and Solvency II capital requirements are, for instance, about 30 % higher for the period with damage data available than for the entire period since the change point. On the other hand, change points are usually harder to detect at the borders of the time series. Thus, the flood frequency regime might have changed recently, without the possibility to detect the respective change point in a statistically significant way.

Regarding the atmospheric drivers of flood events in the Mondsee region within the instrumental period (1976-2013), most of the top 20 daily precipitation extremes in summer (April to August) were found to be related to type Vb cyclones, which develop around Northern Italy south of the Alps. Those top precipitation events correspond very well with the sedimentary Lake Mondsee flood record (up to 80 %). As another main feature, a major Cut-Off Low could be identified at upper atmospheric levels directly located across the Alpine range. In consequence a strong pressure gradient at the surface level leads to an enhanced northerly flow at deep atmospheric layers, favouring extreme precipitation amounts by orographic lifting in this region. The resulting floods, which also trigger sediment deposition in Lake Mondsee, are high intensity floods (e.g. 12.08.2002 and 02.06.2013), presenting highest hourly discharges (> 85 m^3/s) and highest discharges lasting at least 1-3 hours. In contrast, antecedent soil moisture and long-rain floods (e.g. 31.07.1977) seem to be not the main factor characterising the sediment flood record of Lake Mondsee.

For the future (2051-2100 compared to 1956-2005), five out of six considered RCP/model-run combinations of the climate model ECHAM6 indicate an increase in the number of precipitation extremes causing flood layer deposition in Lake Mondsee. Since results also illustrate a mean decrease in the annual number of Vb cyclones for the future, change signals in precipitation extremes are based in the first instance on temperature changes and consequently in changes in humidity available in the atmosphere. The change signals in deposition-causing precipitation extremes translate into expected shifts in average annual damage and Solvency II capital requirements ranging from -19 % to +75 %, assuming no changes in the building stock value. Natural variability is however higher than the shift expected due to climate change. Taking changes in the building stock value into account, the assumed net growth counteracts climate-induced decreases and exacerbates climate-induced increases in the damage potential.

Whereas the considered building stock value scenarios have a comparably small effect on the future average annual damage, they may more than double the climate change effect on the Solvency II capital (99.5 % VaR), especially if construction activities in risk zones are not regulated.

Sensitivity analysis shows that the high temporal resolution of the Lake Mondsee sediment record is of high value. Lower temporal resolution of (sedimentary) flood records can hamper the analysis of relations between flood records and climatic signals. Understanding the interplay between climatic signals and flood occurrences is, however, an important ingredient for proper flood risk estimation and the management of flood risk. To improve the understanding of this interplay, high resolution records with robust chronologies and flood information (e.g. flood seasonality and flood characteristics) are essential.

Other target groups who can draw relevant and interesting conclusions from the project results and continue working on that basis include the Past Global Changes Initiative (PAGES, http://pastglobalchanges.org/). PAGES could use the approach developed in FloodRisk-7000 for evaluating other flood records from natural geoarchives, e.g. understanding paleofloods and related cyclone tracks, change point analysis for investigating changing flood regimes and implementing information in flood risk assessments. The change point approach performed in FloodRisk-7000, for example, enables a comparison to other flood records, and possibly to relate flood frequencies to climatic conditions, by looking for similar change points in the historical record of the latter. We performed a respective statistical analysis for Lake Ammersee (Germany), Lake Ledro (Italy), Lake Savine (France), the sediment thickness series of Lake Bourget (France) and the North Atlantic Oscillation (NAO) time series. In a number of cases, again one significant change point was detected, albeit not at the same time as the one for the Mondsee record. Future studies could hence be directed towards understanding a possibly common mechanism causing such change points. Moreover, it would be of great interest to apply the developed methods on paleoflood records that include information on flood magnitude. The sediment records of Lake Mondsee "only" provide information on the frequency of flood events, but not on their size. This somewhat limits their ability in reducing uncertainties related to the estimation of flood damage potentials.

C) Project details

6 Methodology

FloodRisk-7000 aimed at improving the estimations on flood damage potentials (with a focus on Northern Austria) by making use of and merging different kinds of data sets, including amongst others damage data, pre-instrumental paleoflood records and cyclone tracks with their corresponding precipitation totals (Figure 10). Damage data is in principle the kind of data most suitable to estimate flood damage potentials. However, it exhibits a crucial cutback: the availability of damage data is usually limited to rather short time horizons (i.e. a few decades in the best case), which causes high uncertainties in estimating the damage potential of these low-probability high-impact events. Hence, the idea behind FloodRisk-7000 is to make use of paleoflood records derived from lake sediments to gain additional insights into the (past) distribution of flood events (provided a sufficient linkage between observed damages and flood events as derived from lake sediments) and thus improve estimations on (current) flood damage potentials. To our knowledge, it's for the first time that long-term information on flood frequency derived from (varved) lake sediments and pre-instrumental paleoflood records serves the attempt to improve estimations on flood damage potentials. Moreover, by comparing flood events derived from sediment records and advanced meteorological circulation patterns, atmospheric patterns leading to major sediment loads can be identified and investigated under future climate change conditions. Using the identified atmospheric patterns and related heavy precipitation events as proxy for the occurrence of floods thus allows for the assessment of the future damage potential as well. In addition, by incorporating atmospheric cyclones as triggers for heavy large scale precipitation the link between flood records and damage is fundamentally strengthened.

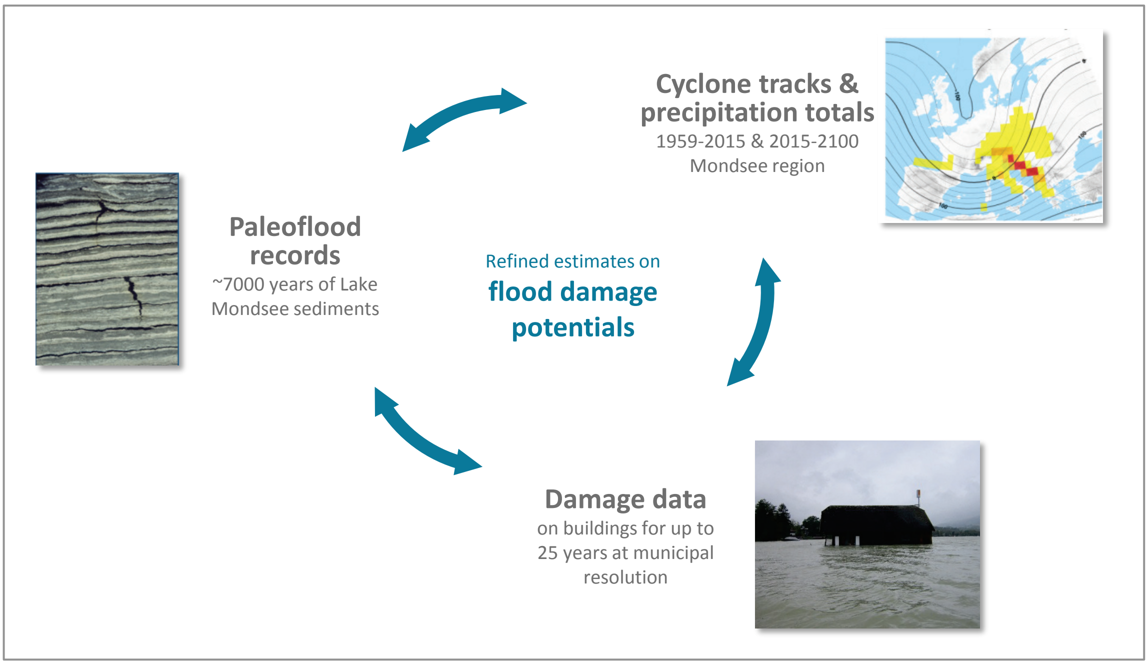

Figure 10: Schematic methodological concept of FloodRiks-7000 (bottom-left picture: Heiko Thoss, GFZ).

What follows is a more detailed description of the methods applied within the single steps and work packages of FloodRisk-7000.

Sediment record analysis (WP1, WP3)

The concept of turbidity currents (Sturm and Matter, 1978) explains the deposition pattern of transported sediment material in lakes during flood events (flood layers). Various studies investigated paleoflood layers of lake sediment sequences so far, but none has either yet linked the flood variability to regional climate boundary conditions or to economic relevant fields. This is mainly due to the limited number of annually laminated (varved) sediment records, which allow quite precise dating these deposited flood layers. Lake Mondsee sediments show a continuous varved sequence with an exceptional record of spring/summer flood layers deposited during the last 7,000 years. The process of flood layer deposition has been investigated at Lake Mondsee in detail during the last years (Lauterbach et al., 2011; Swierczynski et al.; 2013; Kämpf et al., 2014). In FloodRisk-7000 we further analysed the proxy data record in order (i) to refine the proxy data record and providing relevant information for model integration, (ii) to define uncertainty ranges for the use of the data, (iii) to improve calibration with instrumental (meteorological) and historical data, and (vi) to compare with other available regional flood records.

In addition, the statistical properties of the long-term flood frequency derived from Lake Mondsee sediments (7,000 years) were analysed in detail. Knowledge about changes of flood occurrence patterns is important for flood risk estimation of the future. Robust and well-calibrated paleoflood records like those preserved in lake sediments are ideal natural records to investigate flood variability of the past and to use the data for further modelling. Hence, we investigated the properties of the inter-flood times with respect to stationarity and dependence and tested model assumptions on the nature of the stochastic process underlying the occurrence of flood events. This included (i) tests for a homogeneous and inhomogeneous Poisson process, using time transformation techniques, (ii) a change point detection analysis based on both, the mean and variance, as well as cumulative sum of square tests on the variance, (iii) auto-correlation and partial auto-correlation plots as well as empirical copula tests with varying lags in the time series to detect possible dependence and persistence patterns and (iv) the fitting of general phase-type distributions using maximum likelihood techniques via the EM algorithm.

Cyclone tracks and related precipitation totals (WP1, WP4)

As mentioned above, the idea behind incorporating atmospheric cyclones as triggers for heavy large scale precipitation was to strengthen the link between sedimentary flood records and damage data. The cyclone track types used in this study were identified by the classification scheme of Hofstätter et al. (2016 and 2018) developed for the European domain. The tracking scheme has been developed by Murray and Simmonds (1991) and Simmonds et al. (1999). In addition it considers both open and closed systems (Pinto et al., 2005) and allows for splitting and merging of cyclone tracks. Closed systems are localized by finding local pressure minima whereas open systems are localized by identifying local vorticity maxima within open troughs. Cyclones are first identified at time t_n, then a first guess for the position at time t_{n+1} is calculated and finally tracks are identified by scoring the direction and distance between the first guess and all candidate cyclones at time t_{n+1}. For the tracking, geopotential height at the atmospheric level of 700 hPa (Z700) and air pressure at sea surface level (SLP) are used separately. Cyclones are tracked within a domain ranging from 40° W to 50° E at 65° N and 20° W to 40° E at 30° N. In order to avoid entrance/exit problems, splitting and merging are refused near the margin. Weak cyclones and spurious tracks are excluded from the analysis (Hofstätter et al., 2016).

In order to exclude small-scale or spurious cyclones, especially over mountain orography, the data are filtered by a discrete spatial low-pass filter (Freser and von Storch, 2005) that removes any structures smaller than 400 km, relaxes smoothly up to 1,000 km, and lets all large scales pass through (see Hofstätter and Chimani, 2012). Cyclone tracks only refer to those cyclones that are located within a "Track Recognition Zone" over Central Europe (TRZ, 0.5° E–23.9° E and 42.3° N–56.2° N) for at least 18 hours (see Hofstätter et al., 2016 for details). For all other cyclones passing outside of TRZ, a track type cannot be assessed, hence such cyclones were not considered in this study. Following the classification of Hofstätter et al. (2016), together with refinements made in Hofstätter et al. (2018), ten different track types are considered in this study, based on the geographic regions the cyclones traverse before entering Central Europe (Table 7).

Table 7: List of cyclone track types of Hofstätter et al. (2018) and plots of individual cyclone tracks with the point of first detection indicated by red dots at SLP for the ten types (type EA is not shown); arrows indicate the typical propagation for each type; JRA-55, 1959-2015.

Acronym	Type	Plot
Vb	van Bebber's type "five-b"	
EA	Eastern Alpine track	
X-N	Northward propagation, emerging from the northern Adriatic Sea or Mediterranean Sea	
X-S	Southward propagation, emerging from the northern Adriatic Sea or Mediterranean Sea	
MED	Mediterranean	
STR	Subtropical	
ATL	Atlantic	
POL	Polar	
CON	Continental	
TRZ	All tracks emerging within TRZ (except Vb, X-N, X-S)	

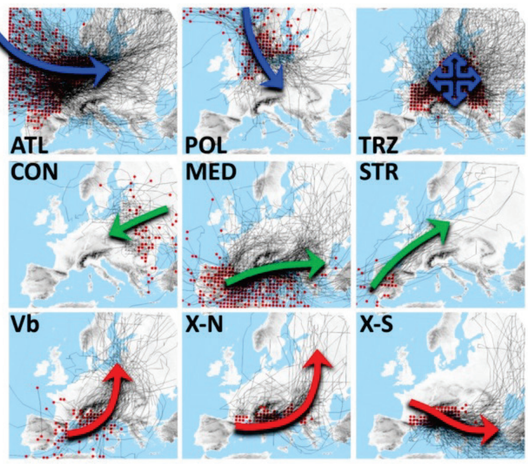

In recent studies (Hofstätter et al., 2018; Messmer et al., 2015; Nissen et al., 2013) specific and dissimilar source and/or target regions were used for identifying Vb tracks, hampering a comparison of results. As the use of source and target regions appears needlessly complicated anyhow and has not been justified so far by physical reasons, a new and less restrictive definition is proposed in this study. All cyclones which propagate northwards at 47° N between 12° E and 22° E are identified as Vb.

In order to attribute individual precipitation events to track types, the 24 hourly precipitation totals (07 MEZ of the current day up to 07 MEZ of the following day) from SPARTACUS (1961-2015) were interpolated to 6 hourly precipitation sums (06, 12, 18 and 00 UTC) for the Mondsee region (R^6). R^6 was assigned to a cyclone track if that cyclone was located within region TRZ at that time. The total precipitation amount of a certain cyclone, denoted as R^{trc}, was determined by summing up precipitation (R^6) as long as a cyclone was within TRZ. In order to further explore individual precipitation events, the 100 largest running 24 hourly precipitation totals (R^{24}) in the period 1961-2015 were identified. A weighted cyclone intensity was calculated for each cyclone, based on the relative geostrophic vorticity and the distance between the cyclone centre and the centre of the respective study region. By this approach cyclones are more likely attributed to a top 100 event at time t, if they are strong and/or if they pass by very close to the respective region.

For analysing changes in extreme precipitation events a statistical model for precipitation simulation using different atmospheric parameters was established. Therefore it was essential to know the parameter to be simulated which turned out to be the maximum 24 hourly precipitation sum (RR^{24max}) during a cyclone track event in TRZ. Moreover, it was important to identify the statistical relations between RR^{24max} and the model input parameters within an extensive test procedure and examination. The following parameter combination turned out to be the most convenient/appropriate: ω^{24} (X_1) and q^{24} (X_2) one time step before RR^{24max} and the square of rh^{24} (X_3) and $grad\_x^{18}$ (X_4) one time step after RR^{24max}, with ω^{24} representing the running 24 hourly weighted average of vertical velocity, q^{24} of specific humidity, rh^{24} of relative humidity, and $grad\_x^{18}$ the running 18 hourly weighted average of the SLP pressure gradient. The formula used for simulating RR^{24max} can be written as follows:

$$RR^{24max} = b_0 + \{b_1 * X_1\} + \{b_2 * X_2\} + \{b_3 * X_3\} + \{b_4 * X_4\} + \{b_5 * (X_1 * X_2)\} + \{b_6 * (X_1 * X_3)\} + \{b_7 * (X_1 * X_4)\}$$

whereby $b_0, \dots, b_7$ are unknown parameters, the so called regression coefficients, determined with help of the available observational (precipitation) and reanalysis data.

Linking of sedimentary flood events with hydro-meteorological data (WP1, WP4)

Daily precipitation and runoff events were compared with flood event layers in Lake Mondsee (1976-2013) and a method for statistically determining probabilities for flood layer deposition in Lake Mondsee based on precipitation events was developed. To establish a method for estimating whether a precipitation event triggers a sedimentary deposition in Lake Mondsee or not, the top 100 list of RR^{24max} was set into relation with flood layer deposition in the lake basin. The 20 largest summer precipitation events (April to August, 1976-2013) in region MSR are correlated to approx. 80 % of flood layer deposition in Lake Mondsee. Finding this correlation allowed to create a simple linear model to estimate probabilities for sedimentary deposition in the lake basin both for the past (JRA-55 and ECHAM6) and for the future (ECHAM6). This makes it possible to define the important threshold for the precipitation amount needed from which on past flood layer depositions were possible. Knowing this value a range from the minimum necessary (corresponds to 0 %) to the maximum possible (corresponds to 100 %) RR^{24max} value in the past was defined for each data set. Hence, the climate change signal in probabilities for sedimentary deposition in Lake Mondsee regarding ECHAM6 could be determined.

Flood damage modelling (WP2, WP3, WP4)

Two different models were used for simulating flood damage, i.e. NeRF_{EVA} and $\text{NeRF}_{\text{HORA}}$, where NeRF represents the abbreviation for Neighbourhood Relationship Flood risk model. Whereas NeRF_{EVA} is based on Extreme Value Analysis (EVA), $\text{NeRF}_{\text{HORA}}$ uses the HORA risk zones as input data.

NeRF_{EVA}: A classical result in the area of Extreme Value Theory due to Fisher and Tippet (1928) states that the distribution of the maxima can only be of one of three types, summarized in the generalized extreme value distribution. Also, the limiting distribution of peaks over high thresholds is of generalized Pareto form, which gives rise to a concrete modelling procedure for large claims. The theory can also be extended to the multivariate case, where the marginal distribution is still a generalized Pareto distribution and the dependence is modelled by extreme value copulas. Hence, following the standard procedure in EVA we fitted a generalized Pareto distribution to the right tail of the distribution of normalized flood damage at municipal level. Since for individual municipalities the time series of available damage data was not sufficiently long to allow for meaningful statistical analysis we chose a model where the number of parameters is reduced. Therefore we assumed that the parameters of the generalized Pareto distribution as well as the threshold (from which on the model is applied) depend on covariates (size of HQ-zones). The spatial dependence of damage between municipalities represents a challenge in the estimation procedure. Following Asadi et al. (2015), who fitted similar models for discharge data, we applied the so called independence likelihood approach (Chandler and Bate, 2007). This approach uses the density of independent random variables in the estimation process, which causes some reduction in efficiency but still leaves the estimator unbiased. Fitting the model to the damage data provided us with a marginal distribution of flood risk for each municipality. To calculate the damage for larger areas, the data needs to be aggregated. For the purpose of aggregation we used a dependence structure estimated from discharge data (see the description of the $\text{NeRF}_{\text{HORA}}$ model below for more details).

$\text{NeRF}_{\text{HORA}}$: In Prettenthaler and Albrecher (2009) a model simulating the yearly damage of floods based on the risk zones of the HORA-database was developed. Whereas in general the marginal distribution of damage in a municipality can reasonably be approximated using the available data from risk maps, it is a challenge to appropriately aggregate zones to the regional or national level, i.e. to specify a dependence model. As regards the model in Prettenthaler and Albrecher (2009), the aggregation was done by two rather ad hoc methods: one approach was to define neighbourhood relationships of adjacent municipalities and regions, and the other approach was based on fitting pre-specified copulas, the type of which were chosen by expert knowledge. The resulting model was quite satisfactory and further modified in the COIN project (Prettenthaler et al., 2015) to predict flood events under changed climatic conditions. However, the dependence modelling was still done in a rather ad hoc manner. In FloodRisk-7000 the original model was enhanced in three aspects:

1. A key input parameter for the model is the average damage to a building. Within FloodRisk-7000 we estimated the damage per building using the damage data at municipal level from the four provinces Salzburg, Upper Austria, Lower Austria and Styria (instead of using figures from the literature).
2. Another key input parameter for the model is the number of buildings located in different risk zones (HORA-zones). For this purpose, we disaggregated data on the built-over area (in m²) from 10 km resolution (Statistics Austria) to 10 m resolution, using satellite data on built-up area from Copernicus European Settlement Map. We assumed one building per 100 m² built-over area.
3. The time series available on flood damage at municipal level are rather short for deriving a spatial dependence structure. However, longer times series are e.g. available on discharge. Since it is arguable that damage caused by flooding is strongly related to events with extreme discharge we can assume that the spatial dependence of extreme discharge is similar to the spatial dependence of flood damage and therefore use the former as a proxy for the latter. Hence, we used data on the river network (from Copernicus) and discharge data from measurement stations (from ehyd) to estimate a max stable process for the dependence of high discharge events in river networks. The method applied is based on Asadi et al. (2015), but splits the area into different regions to account for different climate influences.

Linking sedimentary flood layers to damage data (WP3)

As already mentioned above, damage data is only available for a comparatively short time interval, comprising a rather limited number of extreme flood events. Hence, estimations on the frequency of such extreme flood events are prone to huge uncertainty when solely based on this short time series of damage data. Using sediment records that provide information on the frequency of significant flood events for a period of 7,000 years has the potential to improve the estimation of return periods. Thus, a probabilistic procedure was developed for linking sedimentary flood events to damage data (see page 16 for details). The procedure allows considering statistical properties of 7,000 years of flood frequency when calculating damage potentials, insurance premiums, and capital requirements. Using the flood damage models $NeRF_{EVA}$ and $NeRF_{HORA}$ together with the developed procedure, 10,000 realizations of flood damage were simulated per considered year for the Mondsee region. These simulations formed the basis for calculating actuarially fair insurance premiums and the Solvency II capital requirements for different time periods within the 7,000 years of sediment records (all years, pre-/post change point, last 100 years). Figures resulting from the additional consideration of 7,000 years of flood frequency experience were compared to figures resulting from considering damage data only (the latter representing the outcome of "previous approaches").

Modelling climate change impacts (WP4)

The impacts of climate change on future flood damage potential was modelled by making use of the links between (i) precipitation extremes and sedimentary flood layers (WP1) as well as (ii) sedimentary flood layers and damage data (WP3).

Based on the probability for flood layer deposition calculated for both ECHAM6 emission scenarios (RCP4.5 and RCP8.5) and all available realizations (run1, run2, and run3) for a historic (1956-2005) and a future (2051-2100) period, we simulated the occurrence of a layer deposition (yes/no) for each year in the two periods. Using these simulated layer depositions and the procedure developed for linking sediment records (i.e. layer depositions) and damage data, 10,000 realizations of flood damage were simulated for each year of the two considered periods. Based on these simulations, expected yearly damage and Value at Risk (VaR) figures were calculated for the historic and the future period. The method was applied on five different building stock value scenarios.

7 Work plan and time schedule

Task (T)	Project month																										
	1	2	3	4	5	6	7	8	9	10	11	12	13	14	15	16	17	18	19	20	21	22	23	24	25	26	27
WP0: Project management																											
T0.1-0.5	M0.1											M0.2															M0.3
WP1: Linking floods and climate: Tracking flood events identified in lake sediments and their linkage to atmospheric cyclones																											
T1.1																								M1.3			
T1.2								M1.1		M1.2																	
T1.3																											
WP2: Analysing flood damage data from catastrophe fund payments																											
T2.1																											
T2.2								M2.1																			
T2.3															M2.2												
T2.4															M2.2												
WP3: Calculating damage potential and insurance premium for the current building stock based on observed long-term flood frequency																											
T3.1																											
T3.2																											
T3.3																		M3.1									
T3.4																		M3.2									
WP4: Modelling the future																											
T4.1																							M4.1				
T4.2															M4.2												
T4.3																									M4.3		
WP5: Uncertainty analysis																											
T5.1																								M5.1			
T5.2																		M5.2									
T5.3																										M5.3	
T5.4																											5.4
WP6: Dissemination																											
T6.1-6.3			M6.1																								M6.2 M6.3

Milestones (M):

0.1: Kick-off meeting
0.2: Interim report
0.3: Final report
1.1: Cyclone track catalogue for 1900-2010
1.2: Categorical precipitation data for region Mondsee for 1900-2010
1.3: Proxy data sets (flood frequency) from Lake Mondsee reflecting floods
2.1: Data collection & normalization completed
2.2: Model calibration completed
3.1: Insurance premiums and flood damage potentials for the considered provinces/municipalities available
3.2: Hypothetical Solvency II capital requirements over the last 7,000 years
4.1: Cyclone track catalogue and precipitation event data for 2015-2100
4.2: Scenarios on building stock value development until 2075 completed
4.3: Calculations on future flood damage potential completed
5.1: Flood frequency record with information about different types of uncertainties
5.2: Evaluation of uncertainties related to meteorology/climatology completed
5.3: Description of uncertainties related to flood risk modelling
5.4: Report on the uncertainties of the present approach and the comparison to previous approaches
6.1: Setup of project website completed
6.2: Stakeholder workshop
6.3: Completion of publications to be submitted to peer-reviewed journals

Tasks (T): 0.1: Management of cooperation between all WPs & partners | **0.2:** Knowledge transfer & coordination of scientific findings between all partners | **0.3**: Supervision of the progress of all work packages | **0.4**: Communication & reporting to the Climate and Energy Fund | **0.5**: Organization & coordination of the interim and final report | **1.1**: Flood pattern of Lake Mondsee in regional and spatial context | **1.2:** Cyclone track catalogue & related heavy precipitation events in the past (1900-2010) | **1.3**: Flood variability & climate change | **2.1**: Collection of flood damage data | **2.2**: Normalization of flood damage data | **2.3**: Modelling of flood damage data – Approach 1 | **2.4**: Modelling of flood damage data – Approach 2 | **3.1**: Testing statistical properties of observed long term flood frequency (derived from Lake Mondsee sediments) | **3.2**: Develop a model relating the flood frequency to actual annual claim data | **3.3**: Calculate insurance premiums & compare the results to premiums determined by other previous approaches | **3.4**: Calculate hypothetical capital requirements for the last 7,000 years | **4.1**: Evolution of cyclone tracks, with a particular potential for heavy precipitation events in region Mondsee, according to climate scenarios until 2100 | **4.2**: Generation of different scenarios on the development of the future building stock value (until 2075) | **4.3**: Future flood damage potential | **5.1**: Uncertainties related to sediment record data | **5.2**: Uncertainties related to meteorology/climatology | **5.3**: Uncertainties related to flood risk modelling | **5.4**: Quantifying uncertainty reduction resulting from the current study | **6.1**: Project website | **6.2**: Dissemination of results to the scientific community via peer-reviewed publications & conference contributions | **6.3**: Dissemination of results to stakeholders & the interested public

8 Publications and dissemination activities

Presentations at conferences and workshops

- Oral presentation by Tina Swierczynski at the PAGES-Paleoflood Workshop in Grenoble (France), 27.-30.06.2016; Title: "*Understanding floods and risks of the last 7000 years at Lake Mondsee*"; URL: http://pastglobalchanges.org/download/docs/working_groups/floods/floods-swierczynski.pdf
- Participation at the PAGES Flood Working Group meeting (Side meeting) at 5th PAGES Open Science Meeting in Zaragoza (Spain), 09.-13.05.2017, Discussion for contributions to a White Paper '*For an improvement of our flood knowledge through paleodata*"
- Poster presentation at EGU General Assembly 2017 in Vienna (Austria), 23.–28.04.2017, Title: "*Hydroclimatic variability in the Lake Mondsee region and its relationships with large-scale climate anomaly patterns*" (Presentation by Norel Rimbu, AWI); URL: https://meetingorganizer.copernicus.org/EGU2017/EGU2017-11342.pdf
- Oral presentation by Judith Köberl at the IWI-Workshop in Muggendorf (Conrad Observatorium), 23.05.2017; Title: "*Calculating flood risk with 7000 years of flood frequency data and highly damage relevant cyclone tracks under current & future climatic conditions*"
- Oral presentation by Franz Prettenthaler and Annemarie Lexer at the Austrian Climate Day in Vienna (Austria), 22.-24.05.2017; Title: "*Calculating flood risk with 7000 years of flood frequency data and highly damage relevant cyclone tracks under current & future climatic conditions*"; URL: https://floodrisk.joanneum.at/wp-content/uploads/2016/04/FloodRisk7000_Klimatag.pdf
- Poster presentation by Tina Swierczynski at the Impacts World 2017 Conference in Potsdam (Germany), 11.-13.10.2017; Title: "*Understanding paleofloods for estimating damage loss potential in the future*"; URL: https://floodrisk.joanneum.at/wp-content/uploads/2016/04/Poster_Mondsee_A0_V2_sm.pdf
- Oral presentation by Franz Prettenthaler at the EGU General Assembly 2018 in Vienna (Austria), 08.-13.04.2018; Title: "*Estimating flood damage potentials by linking paleoflood records and empirical loss data*"; URL: https://floodrisk.joanneum.at/wp-content/uploads/2018/04/FloodRisk7000_EGU2018_NH92.pdf
- PICO presentation by Tina Swierczynski at the EGU General Assembly 2018 in Vienna (Austria), 08.-13.04.2018; Title: "*Linking paleofloods to precipitation extremes at Lake Mondsee (NE Alps)*"; URL: https://floodrisk.joanneum.at/wp-content/uploads/2018/06/Linking-paleofloods_EGU2018_update.pdf

Peer-reviewed publications

- Swierczynski, T., Ionita, M., Pino, D. (2017): Using archives of past floods to estimate future flood hazards, Eos, 98. URL: https://eos.org/meeting-reports/using-archives-of-past-floods-to-estimate-future-flood-hazards
- Wilhelm, B., Ballesteros Canovas, J.A., Corella Aznard, J. P., Kämpf, L., Swierczynski, T. Stoffel, M., Støren, E., Toonen, W. (2018): Recent advances in paleoflood hydrology: From new archives to data compilation and analysis, Water Security, 3. URL: https://doi.org/10.1016/j.wasec.2018.07.001
- Swierczynski, T., Lexer, A., Kämpf et al., Prettenthaler, F., Hofstätter, M. (in preparation): Linking paleofloods to daily precipitation extremes at Lake Mondsee (NE Alps).
- Albrecher, H., Kortschak, D., Prettenthaler, F. (in preparation): On spatial dependence modelling of flood risk in Austria.
- Albrecher, H., Bladt, M., Kortschak, D., Prettenthaler, F., Swierczynski, T. (in review): Identification of a change point in the paleoflood record from Lake Mondsee (NE Alps) – Implications for flood risk estimations of the future. (submitted to Global and Planetary Change).
- Hofstätter, M. (in review): Vb cyclones synchronized with the Arctic-/North Atlantic Oscillation. (submitted to Journal of Geophysical Research).
- Prettenthaler, F., Albrecher, H., Bladt, M., Hofstätter, M., Köberl, J., Kortschak, D., Lexer, A., Swierczynski, T. (in preparation): Integrated sediment, climate, and statistical modelling to better understand flood risk.

Other publications

- Wilhelm, B., Ballesteros Canovas, J., Ahlborn, M., Baker, V., Benito, G., Francus, P., Glaser, R., Kahle, M, Mudelsee, M., Carlos Peña, J., Schulte, L. St George, S., Swierczynski, T. (2017): White paper of PAGES Floods Working Group – For an improvement of our flood knowledge through paleodata. URL: http://pastglobalchanges.org/download/docs/working_groups/floods/fwg-white-paper-Nov-17.pdf

Articles on websites and in newspapers

- News article on the website of applicant JOANNEUM RESEARCH, 24.05.2017; Title: "*FloodRisk-7000: Neue Ansätze zur Hochwasserschadenpotentialschätzung – Präsentation beim 18. Österreichischen Klimatag*"; URL: https://www.joanneum.at/life/aktuelles/news/news-detail/news/floodrisk-7000-neue-ansaetze-zur-hochwasserschadenpotentialschaetzung/?tx_news_pi1%5Bcontroller%5D=News&tx_news_pi1%5Baction%5D=detail&cHash=6e1cffa2d49b1340272ebad8918242ab

- News article in "derStandard", following the presentation at the Austrian Climate Day; 24.05.2017; Title: "*Bohrkern aus dem Mondsee liefert Daten aus 7.000 Jahren*"; URL: https://derstandard.at/2000058206473/Bohrkern-aus-dem-Mondsee-liefert-Daten-aus-7-000-Jahren
- News article in "Tiroler Tageszeitung", following the presentation at the Austrian Climate Day; 24.05.2017; Title: "*7.000 Jahre alter Mondseebohrkern soll Hochwassergefahr klären*"; URL: http://www.tt.com/home/13018539-91/7.000-jahre-alter-mondseebohrkern-soll-hochwassergefahr-kl%C3%A4ren.csp
- News article at "steiermark.orf.at", following the presentation at the Austrian Climate Day; Title: "*Mondsee-Bohrkern soll Hochwassergefahr klären*"; URL: http://steiermark.orf.at/news/stories/2845220/

9 Bibliography

Asadi, P., Davison, A.C., Engelke, S. (2015): Extremes on river networks, The Annals of Applied Statistics, 9(4), 2023-2050.

Chandler, R.E., Bate, S. (2007): Inference for clustered data using the independence log-likelihood, Biometrika 94, 167-183.

Fisher, R.A., Tippett, L.H.C. (1928): Limiting forms of the frequency distribution of the largest and smallest member of a sample, Proc. Cambridge Philosophical Society 24,180-190.

Giorgetta, M.A., Roeckner, E., Mauritsen, T., Stevens, B., Crueger, T., Esch, M., Rast, S., Kornblueh, L., Schmidt, H., Kinne, S., Möbis, B., Krismer, T., Reick, C., Raddatz, T., Gayler, V. (2012): The atmospheric general circulation model ECHAM6 - Model description, URL: https://www.mpimet.mpg.de/fileadmin/publikationen/Reports/WEB_BzE_135.pdf

Harada, Y., Kamahori, H., Kobayashi, C., Endo, H., Kobayashi, S., Ota, Y., Onoda, H., Onogi, K., Miyaoka, K., Takahashi, K. (2016): The JRA-55 reanalysis: representation of atmospheric circulation and climate variability. J. Meteorol. Soc. Jpn. 94, 269-302, https://doi.org/10.2151/jmsj.2016-015.

Hofstätter, M., Chimani, B., Lexer, A., Blöschl, G. (2016): A new classification scheme of European cyclone tracks with relevance to precipitation. WaterResour.Res. 52, 7086-7104. https://doi.org/10.1002/2016WR019146.

Hofstätter, M., Lexer, A., Homann, M., Blöschl, G. (2018): Large-scale heavy precipitation over central Europe and the role of atmospheric cyclone track types. Int. J. Climatol 38, 497-517. doi:10.1002/joc.5386

Japanese Meteorological Agency (2013): JRA-55: Japanese 55-year reanalysis, daily 3-hourly and 6-hourly data. Computational and Information Systems Laboratory, National Center for Atmospheric Research: Tokyo (accessed 16 May 2016). https://doi.org/10.5065/D6HH6H41.

Kämpf, L., Brauer, A., Swierczynski, T., Czymzik, M., Mueller, P., Dulski, P. (2014): Processes of flood-triggered detrital layer deposition in the varved Lake Mondsee sediment record revealed by a dual calibration approach, Journal of Quaternary Science, 29 (5), 475-486, https://doi.org/10.1002/jqs.2721

Kobayashi, S., Ota, Y., Harada, Y., Ebita, A., Moriya, M., Onoda, H., Onogi, K., Kamahori, H., Kobayashi, C., Endo, H., Miyaoka, K., Takahashi, K. (2015): The JRA-55 reanalysis: general specifications and basic characteristics. J. Meteorol. Soc. Jpn. 93, 5-48, https://doi.org/10.2151/jmsj.2015-001.

Lauterbach, S., Brauer, A., Andersen, N., Danielopol, D.L., Dulski, P., Hüls, M., Milecka, K., Namiotko, T., Obremska, M., von Grafenstein, U. (2011): Declakes participants: Environmental responses to Lateglacial climatic fluctuations recorded in the sediments of pre-Alpine Lake Mondsee (northeastern Alps). J. Quat. Sci. 26, 253-267.

ÖROK (2015): ÖROK-Regionalprognosen 2014 – Bevölkerung; downloaded from http://www.oerok.gv.at/index.php?id=1152

Prettenthaler, F., Albrecher, H., (Ed.) (2009): Hochwasser und dessen Versicherung in Österreich, Studien zum Klimawandel Band III, Verlag der Österreichischen Akademie der Wissenschaften, Wien, ISBN 978-3-7001-6753-2.

Prettenthaler, F., Kortschak, D., Hochrainer-Stigler, S., et al. (2015): Catastrophe Management: Riverine Flooding, Chapter 18 in Steininger, K. et al. (ed.) Economic Evaluation of Climate Change Impacts: Development of a Cross-Sectoral Framework and Results for Austria, Springer.

Reick, C., et al. (2012a): CMIP5 Simulations of the Max Planck Institute for Meteorology (MPIM) Based on the MPI-ESM-LR Model: The esmHistorical Experiment, Served by ESGF, World Data Cent. for Clim, doi:10.1594/WDCC/CMIP5.MXELeh, WDCC, DKRZ.

Reick, C., et al. (2012b): CMIP5 Simulations of the Max Planck Institute for Meteorology (MPIM) Based on the MPI-ESM-LR Model: The esmrcp85 Experiment, Served by ESGF, World Data Cent. for Clim, doi:10.1594/WDCC/CMIP5.MXELe8.], WDCC, DKRZ.

Sturm, M., Matter, A. (1978): Turbidites and varves in Lake Brienz (Switzerland): Deposition of clastic detritus by density currents. In Modern and Ancient Lake Sediments, A. Matter, and M. E. Tucker, Eds., Blackwell, Oxford. Special Publication of the International Association of Sedimentologists 2, 147-168.

Swierczynski, T., Brauer, A., Lauterbach, S., Martín-Puertas, C., Dulski, P., von Grafenstein, U., Rohr, C. (2012): A 1600-year seasonally resolved record of decadal-scale flood variability from the Austrian pre-Alps, Geology 40, 1047-1050.

Swierczynski, T., Lauterbach, S., Dulski, P., Delgado, J., Merz, B. (2013): Mid- to late Holocene flood frequency changes in the northeastern Alps as recorded in varved sediments of Lake Mondsee (Upper Austria), Quaternary Science Reviews 80, 78-90.

Swierczynski, T., Lauterbach, S., Dulski, P., Brauer, A. (2013): Late Neolithic Mondsee Culture in Austria: living on lakes and living with flood risk? Climate of the Past 9, 1601-1612.

Swierczynski, T., Lexer, A., Kämpf et al., Prettenthaler, F., Hofstätter, M. (in preparation): Linking paleofloods to daily precipitation extremes at Lake Mondsee (NE Alps).

Details "ECHAM6" (MPI-ESM-LR)

Data Owner: Max Planck Institute for Meteorology

data-ID for historical runs: project=CMIP5, model=MPI-ESM-LR, Max Planck Institute for Meteorology (MPI-M), experiment=historical, time_frequency=6hr, modeling realm=atmos, ensemble=r1i1p1 & r2i1p1 & r3i1p1 version=20111006 data-ID for future simulations: project=CMIP5, model=MPI-ESM-LR, Max Planck Institute for Meteorology (MPI-M), experiment=RCP4.5 & RCP8.5, time_frequency=6hr, modeling realm=atmos, ensemble=r1i1p1 & r2i1p1 & r3i1p1, version=20111006

retrieved from: Earth System Grid Federation (World Climate Research Programme): http://cmippcmdi.llnl.gov/cmip5/data_portal.html

“We acknowledge the World Climate Research Programme's Working Group on Coupled Modelling, which is responsible for CMIP, and we thank the climate modeling groups (Max Planck Institute for Meteorology; EC-Earth Consortium) for producing and making available their model output. For CMIP the U.S. Department of Energy's Program for Climate Model Diagnosis and Intercomparison provides coordinating support and led development of software infrastructure in partnership with the Global Organization for Earth System Science Portals.”

CMIP5 Coupled Model Intercomparison Project: http://cmip-pcmdi.llnl.gov/cmip5

Diese Projektbeschreibung wurde von der Fördernehmerin/dem Fördernehmer erstellt. Für die Richtigkeit, Vollständigkeit und Aktualität der Inhalte sowie die barrierefreie Gestaltung der Projektbeschreibung, übernimmt der Klima- und Energiefonds keine Haftung.

Die Fördernehmerin / der Fördernehmer erklärt mit Übermittlung der Projektbeschreibung ausdrücklich über die Rechte am bereitgestellten Bildmaterial frei zu verfügen und dem Klima- und Energiefonds das unentgeltliche, nicht exklusive, zeitlich und örtlich unbeschränkte sowie unwiderrufliche Recht einräumen zu können, das Bildmaterial auf jede bekannte und zukünftig bekanntwerdende Verwertungsart zu nutzen. Für den Fall einer Inanspruchnahme des Klima- und Energiefonds durch Dritte, die die Rechtinhaberschaft am Bildmaterial behaupten, verpflichtet sich die Fördernehmerin / der Fördernehmer den Klima- und Energiefonds vollumfänglich schad- und klaglos zu halten.